CHEMISTRY
A EUROPEAN JOURNAL

DOI: 10.1002/chem.200500814

Hydrocarbon Oxidation by β-Halogenated Dioxoruthenium(VI) Porphyrin Complexes: Effect of Reduction Potential ($Ru^{VI/V}$) and C–H Bond-Dissociation Energy on Rate Constants

Chi-Ming Che,*[a] Jun-Long Zhang,[a] Rui Zhang,[a] Jie-Sheng Huang,[a] Tat-Shing Lai,[b] Wai-Man Tsui,[a] Xiang-Ge Zhou,[a] Zhong-Yuan Zhou,[c] Nianyong Zhu,[a] and Chi Kwong Chang[b]

Abstract: β-Halogenated dioxoruthenium(VI) porphyrin complexes [Ru^{VI}-(F_{28}-tpp)O_2] [F_{28}-tpp = 2,3,7,8,12,13,17,18-octafluoro-5,10,15,20-tetrakis-(pentafluorophenyl)porphyrinato(2−)] and [Ru^{VI}(β-Br_8-tmp)O_2] [β-Br_8-tmp = 2,3,7,8,12,13,17,18-octabromo-5,10,15,20-tetrakis(2,4,6-trimethylphenyl)porphyrinato(2−)] were prepared from reactions of [Ru^{II}(por)(CO)] [por = porphyrinato(2−)] with *m*-chloroperoxybenzoic acid in CH_2Cl_2. Reactions of [Ru^{VI}(por)O_2] with excess PPh_3 in CH_2Cl_2 gave [Ru^{II}(F_{20}-tpp)(PPh_3)$_2$] [F_{20}-tpp = 5,10,15,20-tetrakis(pentafluorophenyl)porphyrinato(2−)] and [Ru^{II}-(F_{28}-tpp)(PPh_3)$_2$]. The structures of [Ru^{II}(por)(CO)(H_2O)] and [Ru^{II}(por)-(PPh_3)$_2$] (por = F_{20}-tpp, F_{28}-tpp) were determined by X-ray crystallography, revealing the effect of β-fluorination of the porphyrin ligand on the coordination of axial ligands to ruthenium atom. The X-ray crystal structure of [Ru^{VI}(F_{20}-tpp)O_2] shows a Ru=O bond length of 1.718(3) Å. Electrochemical reduction of [Ru^{VI}(por)O_2] (Ru^{VI} to Ru^{V}) is irreversible or quasi-reversible, with the $E_{p,c}(Ru^{VI/V})$ spanning −0.31 to −1.15 V versus $Cp_2Fe^{+/0}$. Kinetic studies were performed for the reactions of various [Ru^{VI}(por)O_2], including [Ru^{VI}-(F_{28}-tpp)O_2] and [Ru^{VI}(β-Br_8-tmp)O_2], with *para*-substituted styrenes *p*-X–$C_6H_4CH{=}CH_2$ (X = H, F, Cl, Me, MeO), *cis*- and *trans*-β-methylstyrene, cyclohexene, norbornene, ethylbenzene, cumene, 9,10-dihydroanthracene, xanthene, and fluorene. The second-order rate constants (k_2) obtained for the hydrocarbon oxidations by [Ru^{VI}-(F_{28}-tpp)O_2] are up to 28-fold larger than by [Ru^{VI}(F_{20}-tpp)O_2]. Dual-parameter Hammett correlation implies that the styrene oxidation by [Ru^{VI}(F_{28}-tpp)O_2] should involve rate-limiting generation of a benzylic radical intermediate, and the spin delocalization effect is more important than the polar effect. The k_2 values for the oxidation of styrene and ethylbenzene by [Ru^{VI}-(por)O_2] increase with $E_{p,c}(Ru^{VI/V})$, and there is a linear correlation between $\log k_2$ and $E_{p,c}(Ru^{VI/V})$. The small slope ($\approx 2\ V^{-1}$) of the $\log k_2$ versus $E_{p,c}(Ru^{VI/V})$ plot suggests that the extent of charge transfer is small in the rate-determining step of the hydrocarbon oxidations. The rate constants correlate well with the C–H bond dissociation energies, in favor of a hydrogen-atom abstraction mechanism.

Keywords: electrochemistry · oxidation · porphyrinoids · ruthenium · structure elucidation

[a] Prof. C.-M. Che, J.-L. Zhang, Dr. R. Zhang, Dr. J.-S. Huang, W.-M. Tsui, Dr. X.-G. Zhou, Dr. N. Zhu
Department of Chemistry and
Open Laboratory of Chemical Biology of the
Institute of Molecular Technology for Drug Discovery and Synthesis
The University of Hong Kong, Pokfulam Road (Hong Kong)
Fax: (+852) 2857-1586
E-mail: cmche@hku.hk

[b] Dr. T.-S. Lai, Prof. C. K. Chang
Department of Chemistry
The Hong Kong University of Science and Technology
Clear Water Bay, Kowloon (Hong Kong)

[c] Prof. Z.-Y. Zhou
Department of Applied Biology and Chemical Technology
The Hong Kong Polytechnic University
Hung Hom, Kowloon (Hong Kong)

Introduction

The discovery that iron porphyrin complexes such as [Fe^{III}(tpp)Cl][1] (tpp = tetraphenylporphyrinato(2−)) can catalyze alkene epoxidation/alkane hydroxylation with PhIO (which mimics the activity of cytochrome P-450 enzymes in biological systems)[2] has stimulated a great deal of interest in metalloporphyrin-catalyzed hydrocarbon oxidation reactions, leading to the development of a wide variety of metalloporphyrin catalysts.[3] A major class of these catalysts is the halogenated metallotetraphenylporphyrin complexes,[4] which bear halogen substituents on the *meso*-phenyl groups (phenyl halogenation) or on the pyrrole groups (β-halogenation) of the porphyrin ligand. The phenyl-halogenated catalysts, such as [M^{III}(F_{20}-tpp)Cl] (M = Fe, Mn; F_{20}-tpp = 5,10,15,20-tetrakis(pentafluorophenyl)porphyrinato(2−))[5] and [Fe^{III}(2,6-Cl_2tpp)Cl] (2,6-Cl_2tpp = 5,10,15,20-tetrakis(2,6-dichlorophenyl)porphyrinato(2−)),[6] exhibit greatly enhanced stability and reactivity toward hydrocarbon oxidations (especially alkene epoxidations) relative to their tpp counterparts. The β-halogenated catalysts, initially designed to further increase the catalyst stability toward hydrocarbon oxidations,[7] show even greater efficiency in catalyzing hydrocarbon oxidations (especially alkane hydroxylations).[8–15] For example, [Fe^{III}(β-Br_8-F_{20}-tpp)Cl] (β-Br_8-F_{20}-tpp = 2,3,7,8,12,13,17,18-octabromo-5,10,15,20-tetrakis(pentafluorophenyl)porphyrinato(2−)) is a remarkably active catalyst for hydroxylation of light alkanes with O_2.[8,11] [M^{III}(β-X_8-2,6-Cl_2tpp)Cl] (M = Fe/Mn, X = Br/Cl/F) catalyze the PhIO hydroxylation of pentane or cyclohexane in considerably higher yields than [M^{III}(2,6-Cl_2tpp)Cl] (M = Fe/Mn).[10,12,16]

To account for the β-halogenation-induced improvement of catalyst efficiency, a number of investigations on the effect of β-halogen substituents on the electronic properties of metalloporphyrin complexes have been reported. Electrochemical measurements[17–20] disclosed that β-halogenation causes a large anodic shift in the redox potentials of the porphyrin complexes.[21] Quantum chemical studies and/or X-ray photoelectron spectroscopy (XPS)/ultraviolet photoemission spectroscopy (UPS)[22] showed that upon β-halogenation the energy of the highest occupied molecular orbital (HOMO) of the porphyrin becomes significantly lower[21] and the porphyrin's lowest ionization potential (IP) becomes markedly higher. These rationalize the smaller susceptibility of β-halogenated catalysts to oxidative degradation. On the other hand, gas-phase electron affinity (EA) measurements[23] revealed that β-halogenated metalloporphyrin complexes exhibit considerably higher EAs than their tpp counterparts. It has been proposed that the enhanced reactivity due to β-halogenation stems from the increase in the electrophilicity of the putative oxometalloporphyrin reactive intermediates.[4,8b,9,23]

Given the proposed reactivity enhancement of an oxometalloporphyrin through β-halogenation, it would be of particular interest to directly examine the effect of β-halogen substituents on the rate constants of the reactions between oxometalloporphyrin complexes and hydrocarbons. This relies on the direct observation or, ideally, the isolation of a β-halogenated oxometalloporphyrin that is reactive toward hydrocarbon oxidations. While a considerable number of reactive oxometalloporphyrin complexes, such as oxochromium(v),[24] oxoiron(iv),[25] oxomanganese(iv/v),[26] and dioxoruthenium(vi) porphyrin complexes,[27] are known in the literature, these reported oxometalloporphyrin complexes invariably bear porphyrin ligands without any β-halogen substituents.[28]

In this paper, we report the isolation and electrochemical properties of two β-halogenated dioxoruthenium(vi) porphyrin complexes and kinetic studies on their reactions with hydrocarbons, together with X-ray crystal structures and electrochemical properties of related carbonylruthenium(ii), bis(triphenylphosphane)ruthenium(ii), and dioxoruthenium(vi) porphyrin complexes. The rate constants obtained for the β-halogenated dioxoruthenium(vi) porphyrin complexes are compared with those of the corresponding β-hydrogenated counterparts, revealing a remarkable rate acceleration by β-halogenation. This is the first direct experimental evidence for the increase in reactivity of an oxometalloporphyrin toward hydrocarbon oxidations by β-halogenation and could be compared with the small rate acceleration due to saddle distortion of the porphyrin ligand observed for the hydrocarbon oxidations by the β-phenylated dioxoruthenium(vi) porphyrin [Ru^{VI}(β-Ph_8-tpp)O_2] (β-Ph_8-tpp = 2,3,5,7,8,10,12,13,15,17,18,20-dodecaphenylporphyrinato(2−)) as reported in previous work.[27e,f] Studies of the linear free-energy relationship between rate constants and thermodynamic driving force showed that the second-order rate constants k_2 for the oxidation of styrene and ethylbenzene by [Ru^{VI}(por)O_2] increase with the reduction potential of Ru^{VI} to Ru^{V}. The rate constants for hydrogen-atom abstraction correlate well with the bond dissociation energy (BDE) of the C–H bond that is cleaved; this result is in accord with previous work on hydrogen-atom abstraction reactions by Mayer and co-workers.[29]

Results

The following porphyrin ligands were employed in this work: 5,10,15,20-(tetraphenylporphyrinato(2−) (tpp; **a**), 5,10,15,20-tetrakis(pentafluorophenyl)porphyrinato(2−) (F_{20}-tpp; **b**), 2,3,7,8,12,13,17,18-octafluoro-5,10,15,20-tetrakis(pentafluorophenyl)porphyrinato(2−) (F_{28}-tpp; **c**), 5,10,15,20-tetrakis(2,4,6-trimethylphenyl)porphyrinato(2−) (tmp; **d**), 2,3,7,8,12,13,17,18-octabromo-5,10,15,20-tetrakis(2,4,6-trimethylphenyl)porphyrinato(2−) (β-Br_8-tmp; **e**) and 5,10,15,20-tetrakis[(1*S*,4*R*,5*R*,8*S*)-1,2,3,4,5,6,7,8-octahydro-1,4:5,8-dimethanoanthracen-9-yl]porphyrinato(2−) (D_4-por*; **f**). Of these ligands, ligand **a** is a sterically unencumbered porphyrin, whereas ligands **d**–**f** are all typical sterically encumbered porphyrins due to the presence of relatively large substituents on the *ortho*-positions of the *meso*-phenyl groups. The perfluorination of ligand **a** leads to the formation the so-called "Teflon" porphyrin **c**. Because fluorine

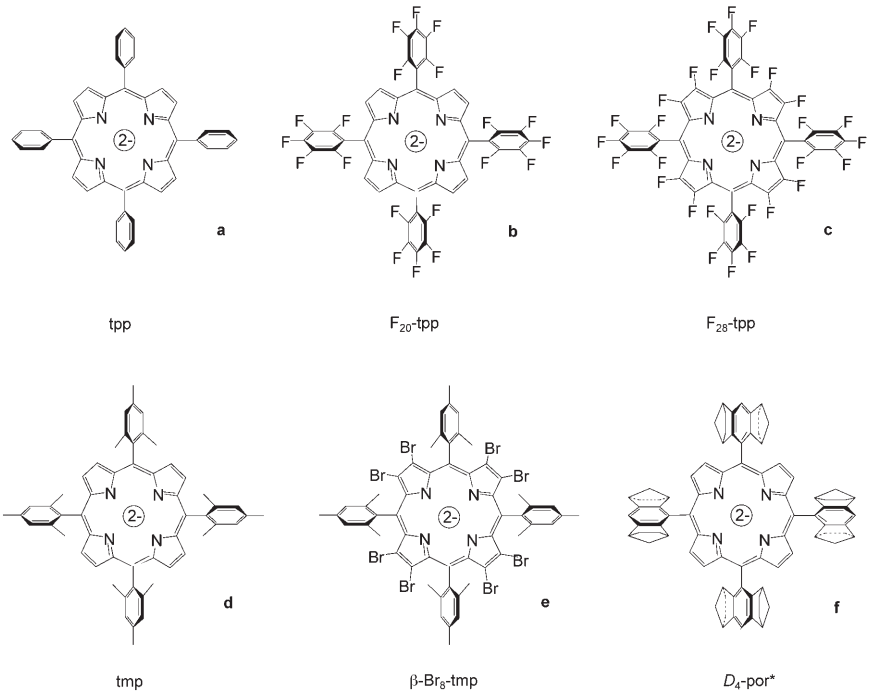

atoms are relatively small, both ligands **b** and **c** are considered essentially sterically unencumbered.

Synthesis and characterization of β-halogenated carbonylruthenium(II), dioxoruthenium(VI), and bis(triphenylphosphane)ruthenium(II) porphyrin complexes

Synthesis: Treatment of $[Ru_3(CO)_{12}]$ with the β-halogenated porphyrin free bases H_2(por) (por = F_{28}-tpp, β-Br_8-tmp) in refluxing 1,2,4-trichlorobenzene under an inert atmosphere resulted in insertion of ruthenium into the porphyrin ligands, affording $[Ru^{II}$(por)(CO)] (por = F_{28}-tpp **1c**, β-Br_8-tmp **1e**) in up to 96% yields. Previously, a number of $[Ru^{II}$(por)(CO)] complexes, including $[Ru^{II}$(tpp)(CO)] (**1a**),[30] $[Ru^{II}(F_{20}$-tpp)(CO)] (**1b**),[31] $[Ru^{II}$(tmp)(CO)] (**1d**),[32] $[Ru^{II}(D_4$-por*)(CO)] (**1f**),[33] and the β-halogenated species $[Ru^{II}(\beta\text{-}X_8\text{-}F_{20}$-tpp)(CO)] (X = Cl, Br),[34] have been prepared from $[Ru_3(CO)_{12}]$ and the respective porphyrin free bases in solvents such as benzene, toluene, decalin, or perfluorobenzene. In this work, we found that 1,2,4-trichlorobenzene is the solvent of choice for the preparation of **1b**,**c**,**e**. The insertion of ruthenium into F_{28}-tpp appears rather difficult: only a 38% yield of **1c** was obtained.

Oxidation of **1b**,**c**,**e** with *m*-chloroperoxybenzoic acid (*m*-CPBA) in CH_2Cl_2 at room temperature afforded the corresponding $[Ru^{VI}$(por)$O_2]$ (por = F_{20}-tpp **2b**, F_{28}-tpp **2c**, β-Br_8-tmp **2e**) in up to 90% yields. Prior to this work, a number of other dioxoruthenium(VI) porphyrin complexes, including $[Ru^{VI}$(tpp)$O_2]$ (**2a**),[27b] $[Ru^{VI}$(tmp)$O_2]$ (**2d**),[27a,32b] and $[Ru^{VI}(D_4$-por*)$O_2]$ (**2f**),[27d] were prepared from reactions of their carbonyl precursors with *m*-CPBA; **2f** has previously been characterized by X-ray crystal-structure determination.[27d]

The β-halogenated dioxoruthenium(VI) complexes **2c**,**e** are less stable than the phenyl-fluorinated species **2b** (which can be stored at −20 °C for months). However, they still exhibit remarkable stability. For example, both **2c**,**e** could be generated in solutions open to air at room temperature and are sufficiently stable for purification by flash chromatography on alumina column, and finally isolated as a spectroscopically pure solid that can be handed at room temperature under air. In contrast, previously reported oxoiron(IV) porphyrin radical cations could not be isolated in solid form at room temperature.[25]

Treatment of **2b**,**c** with an excess of triphenylphosphane in CH_2Cl_2 afforded $[Ru^{II}$(por)$(PPh_3)_2]$ (por = F_{20}-tpp **3b**, F_{28}-tpp **3c**) as a dark purple solid in 78 and 80% yields, respectively, after washing with ethanol.

Spectroscopy: Complexes **1c**,**e**, **2b**,**c**,**e**, and **3b**,**c** were characterized by NMR, IR, and UV-visible spectroscopy, along with mass spectrometry. A detailed compilation of the spectral data is given in the Experimental Section.

The positive-ion mass spectra of **1c**,**e** and **2b**,**c**,**e** show cluster peaks attributable to the parent ions $[M^+]$ and the fragments $[M^+-L]$ (L = O or CO). Other cluster peaks corresponding to the fragments $[M^+-2O]$ for **2b**,**c**,**e** are also present. For **3b**,**c**, the positive-ion FAB mass spectra show cluster peaks attributable to the fragments $[M^+-PPh_3]$ and $[M^+-2PPh_3]$. The ν(CO) bands of **1c**,**e** in the IR spectra (1996 (**1c**) and 1954 (**1e**) cm^{-1}) are at comparable frequencies to those of their β-hydrogenated counterparts **1b** (1965 cm^{-1})[31b] and **1d** (1940 cm^{-1}),[32b] respectively.[35] Complexes **2b**,**c**,**e** exhibit ν(RuO) bands at 826, 823, and 824 cm^{-1}, respectively, similar to those previously reported for **2a** (819 cm^{-1}),[27c] **2d** (821 cm^{-1}),[32b] and **2f** (822 cm^{-1}).[27d]

In UV-visible spectra, the Soret band of carbonyl- and bis(triphenylphosphane)ruthenium(II) fluorinated porphyrin complexes **1c** and **3b**,**c** appears at 394–413 nm, whereas that of carbonylruthenium(II) β-brominated porphyrin **1e** is red-shifted to 430 nm. For dioxoruthenium(VI) porphyrin complexes, the Soret band is located at 399–412 nm (fluorinated porphyrin complexes **2b**,**c**) and 456 nm (β-brominated porphyrin complex **2e**). The β-band appears at 498–516 nm for **1c** and **3b**,**c**, 560 nm for **1e**, 494–506 nm for **2b**,**c**, and 540 nm for **2e**. On going from **1c** to **2c**, or from **1e** to **2e**, a considerable red-shift of the Soret band and blue-shift of the β-band were observed, similar to that of the reported

carbonylruthenium(II) and dioxoruthenium(VI) porphyrin complexes.[27]

The ^{1}H NMR spectrum of **2b** shows the signal of β-H (the pyrrolic protons of the porphyrin ligand) at 9.18 ppm, which is downfield from that of **1b** (8.70 ppm).[31b] In the case of **2e**, the signal of the *meso*-phenyl protons appears at 7.20 ppm, comparable to that of **1e** (7.18 ppm). Complexes **3b**,**c** have axial phenyl signals at 6.77 (*p*-H)/6.47 (*m*-H)/4.30 (*o*-H), and 6.95 (*p*-H)/6.66 (*m*-H)/4.57 ppm (*o*-H), respectively; the β-H signal of **3b** appears at 8.08 ppm.

Complexes **2b**,**c** and **3b**,**c** have ^{19}F NMR signals at −135.4 to −138.4 (*o*-F), −148.9 to −153.7 (*p*-F), and −160.9 to −162.9 ppm (*m*-F), respectively, with the β-F signal appearing at −143.3 (**2c**) and −145.3 ppm (**3c**). All the signals of **2b**,**c**, except the *o*-F signals, are downfield from the corresponding signals of **3b**,**c**. The ^{19}F NMR spectra of **1b**,**c** each have two *o*-F signals (≈ −138 and −139 ppm) and two *m*-F signals (≈ −160 and −161 ppm), consistent with the unsymmetrical axial coordination in both complexes. The β-F signal of **1c** at −144.6 ppm falls between those of **2c** and **3c**. In the ^{31}P NMR spectra of **3b**,**c**, the signal of axial phosphane ligands appears at 5.61 and 4.59 ppm, respectively. Both **3b**,**c** are stable in $CDCl_3$ and we observed no dissociation of axial PPh_3 ligands after 24 h.

X-ray crystal structures: We have determined the structures of **1b**·H_2O·2CH_2Cl_2, **1c**·4H_2O·MeOH, **2b**·2 MeOH, and **3b**,**c** by X-ray crystallography; the respective ORTEP drawings are depicted in Figures 1–5. Complexes **1c**·4 H_2O·MeOH and **3c** are the first structurally characterized ruthenium complexes bearing an F_{28}-tpp ligand,[36] whereas **2b** is the only dioxoruthenium(VI) sterically unencumbered porphyrin complex, with its structure determined by X-ray crystal analysis.

The porphyrin rings in **1b**,**c**, **2b**, and **3b** are essentially planar, with the mean deviation of 0.055, 0.031, 0.019, and 0.046 Å, respectively. For **3c**, an appreciable puckering of the porphyrin ring is observed (mean deviation: 0.089 Å), and the largest displacement from the mean plane is 0.158 Å. The ruthenium atom in **2b** and **3b**,**c** is situated in the porphyrin plane, but that in **1b**,**c** is 0.0032 and 0.0517 Å, respectively, out of the mean plane of the porphyrin ring toward the carbonyl group.

Both **1b**,**c** bind a water molecule at an axial site in the crystal structure (Figure 1, selected bond lengths and angles are given in Table 1).[37] The structure of **1b**·H_2O·2CH_2Cl_2 features a long Ru−C(CO) bond of 1.923(5) Å coupled with a short C−O bond of 1.018(7) Å [compared with the Ru−C(CO) bonds of 1.77(2)–1.838(9) Å and the C−O bonds of 1.13(2)–1.18(3) Å in other β-hydrogenated carbonylruthenium(II) porphyrin complexes[30b,d,35c–35f,38,39]], and a long Ru−O(H_2O) distance of 2.459(4) Å [compared with that of 2.172–2.291(8) Å in [Ru^{II}(por)(CO)]·H_2O (por = oep,[40] tmp[35d]) and [Ru^{II}(β-Cl_8-F_{20}-tpp)(CO)]·H_2O·2 AcOEt[34]). The corresponding geometric parameters in **1c**·4H_2O·MeOH are normal [Ru−C(CO) 1.832(4) Å, C−O 1.121(5) Å, Ru−O(H_2O) 2.268(4) Å] and are comparable to those of [Ru^{II}(β-Cl_8-F_{20}-tpp)(CO)]·H_2O·2 AcOEt.[34] There is

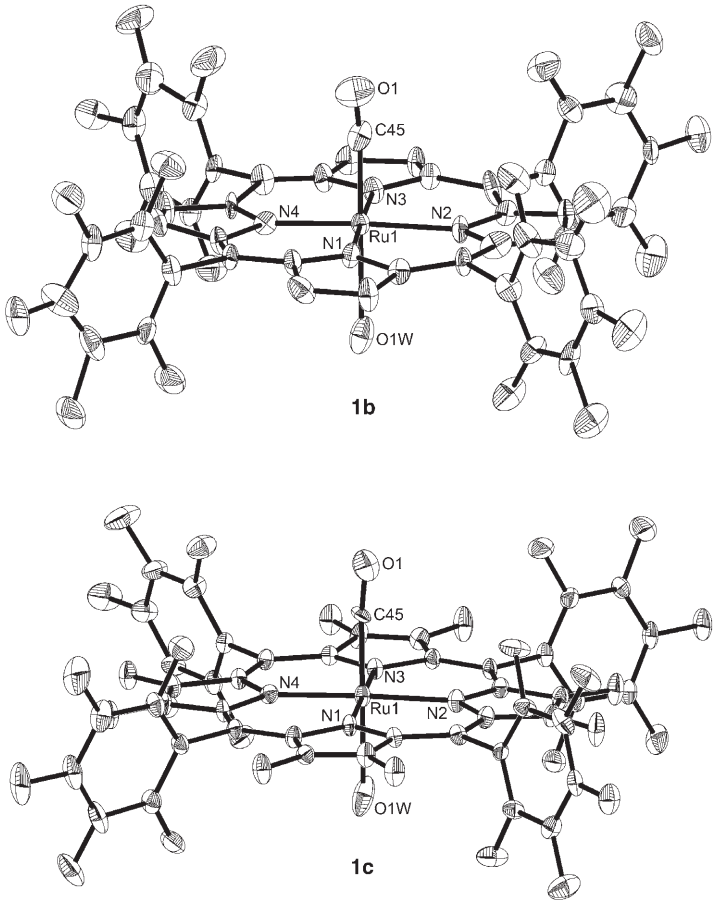

Figure 1. ORTEP drawings of **1b**·H_2O·2 CH_2Cl_2 and **1c**·4H_2O·MeOH with the atom-numbering scheme. Hydrogen atoms and the uncoordinated solvent molecules are not shown.

Table 1. Selected bond lengths [Å] and angles [°] for **1b**·H_2O·2 CH_2Cl_2 and **1c**·4H_2O·MeOH.

	1b·H_2O·2 CH_2Cl_2	**1c**·4H_2O·MeOH		**1b**·H_2O·2 CH_2Cl_2	**1c**·4H_2O·MeOH
Ru1−N1	2.065(3)	2.050(3)	Ru1−N2	2.097(3)	2.048(3)
Ru1−N3	2.044(3)	2.032(3)	Ru1−N4	2.002(2)	2.041(3)
Ru1−C45	1.923(5)	1.832(4)	Ru1−O1W	2.459(4)	2.268(4)
C45−O1	1.018(7)	1.121(5)			
Ru1-C45-O1	171.8(5)	173.4(4)	C45-Ru1-O1W	178.9(2)	179.3(1)
C45-Ru1-N1	90.5(2)	91.4(1)	C45-Ru1-N2	91.7(2)	91.8(1)
C45-Ru1-N3	88.2(2)	90.1(1)	C45-Ru1-N4	91.8(2)	90.5(1)
O1W-Ru1-N1	90.5(1)	88.3(1)	O1W-Ru1-N2	88.3(1)	88.8(1)
O1W-Ru1-N3	90.8(1)	90.2(1)	O1W-Ru1-N4	88.2(1)	88.9(1)
N1-Ru1-N2	88.9(1)	89.7(1)	N2-Ru1-N3	89.1(1)	90.6(1)
N3-Ru1-N4	90.0(1)	89.6(1)	N4-Ru1-N1	92.1(1)	90.1(1)
N1-Ru1-N3	177.6(1)	178.4(1)	N2-Ru1-N4	176.4(1)	177.7(1)

an interporphyrin hydrogen-bonding interaction between the CO and H_2O axial ligands of adjacent molecules in the crystal structure of **1b**·H_2O·2CH_2Cl_2; this results in a polymeric one-dimensional chain structure as shown in Figure 2 with O···O distances of 2.779 Å.[41]

Complex **2b** (Figure 3, selected bond lengths and angles are given in Table 2) has a linear O=Ru=O moiety (O1-Ru1-O1′ 180.0(1)°) perpendicular to the porphyrin ring plane, along with two types of intermolecular hydrogen bonds: one is between a β-C–H bond and an oxo group (C···O 3.189 Å), the other is between a β-C–H bond and a *p*-F atom of the *meso*-phenyl group (C···F 3.344 Å) (Figure 4). The Ru=O bond lengths in **2b** are 1.718(3) Å, slightly shorter than those of 1.73(1) and 1.75(1) Å in **2f**[27d] (this can be attributed to the electron-withdrawing effect of the fluoro group) and are comparable to those of 1.705(7) and 1.718(5) Å in *trans*-[Ru^{VI}(16-tmc)O_2](ClO_4)$_2$ (16-tm*c* = 1,5,9,13-tetramethyl-1,5,9,13-tetraazacyclohexadecane)[42] and *trans*-[Ru^{VI}(15-tmc)O_2](ClO_4)$_2$ (15-tmc = 1,4,8,12-tetramethyl-1,4,8,12-tetraazacyclopentadecane),[42] respectively.

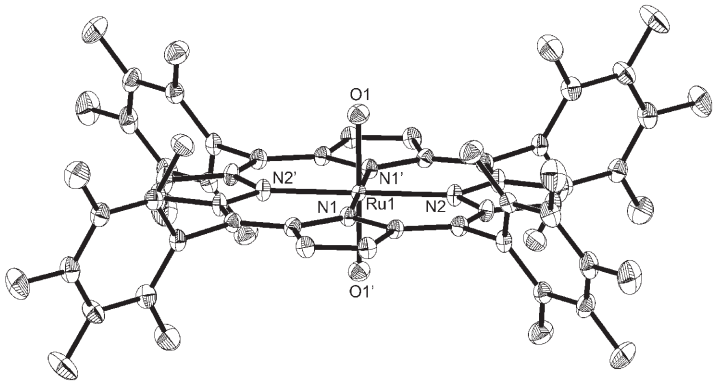

Figure 3. ORTEP drawing of **2b**·2MeOH with the atom-numbering scheme. Hydrogen atoms and the solvent molecules are not shown.

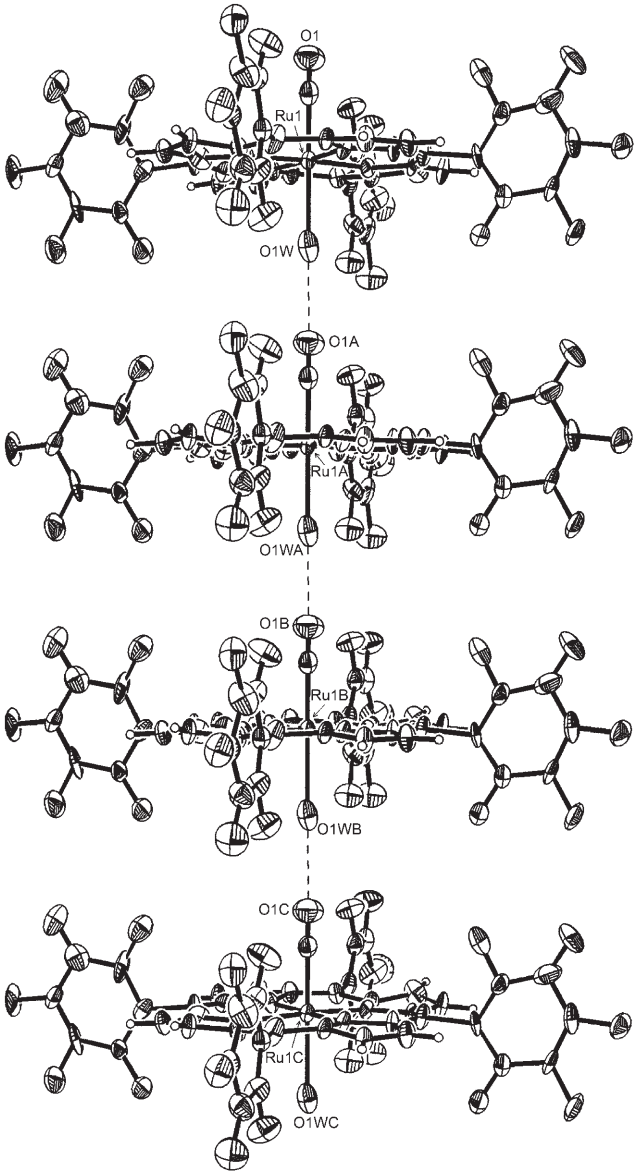

Figure 2. Interporphyrin O(CO)···O(H_2O) hydrogen bonding in **1b**·H_2O·2CH_2Cl_2.

Table 2. Selected bond lengths [Å] and angles [°] for **2b**·2MeOH.

Ru1–N1	2.066(3)	Ru1–N2	2.057(3)
Ru1–N1′	2.066(3)	Ru1–N2′	2.057(3)
Ru1–O1	1.718(3)	Ru1–O1′	1.718(3)
O1-Ru1-O1′	180.0(1)	O1-Ru1-N1	90.94(13)
O1-Ru1-N2	89.73(13)	O1-Ru1-N1′	89.06(13)
O1-Ru1-N2′	90.27(13)	O1′-Ru1-N1	89.06(13)
O1′-Ru1-N2	90.27(13)	O1′-Ru1-N1′	90.94(13)
O1′-Ru1-N2′	89.73(13)	N1-Ru1-N2	90.02(12)
N1-Ru1-N1′	180.0(2)	N1-Ru1-N2′	89.98(12)
N1′-Ru1-N2′	90.02(12)	N2-Ru1-N1′	89.98(12)
N2-Ru1-N2′	180.0		

The structure of **3b**,**c** features a linear P-Ru-P moiety (P1-Ru1-P1′ 180°), which is perpendicular to the porphyrin ring plane (Figure 5, selected bond lengths and angles are given in Table 3). The Ru–P bond lengths of 2.4643(9) Å in **3b** and 2.4807(7) Å in **3c** are longer than that of 2.297(5)–2.428 Å in previously reported bis(tertiary phosphane)ruthenium(II) porphyrin complexes.[43]

Electrochemical studies: Cyclic voltammetry was used to examine the electrochemical properties of **1c**, **2a**–**f**, [Ru^{VI}(ttp)O_2] (**2g**), [Ru^{II}(tpp)(PPh_3)$_2$] (**3a**), and **3b**,**c** in CH_2Cl_2. The redox potentials (V versus $Cp_2Fe^{+/0}$) are listed in Table 4. Selected cyclic voltammograms are shown in Figures 6 and 7. Complexes **2a**,**b**,**d**–**g**, and **3a**,**b** show one reversible or quasi-reversible oxidation couple with $E_{1/2}$ = 0.60–1.33 V, which is assigned to oxidation of the porphyrin ligands. As expected, for the complexes bearing F_{28}-tpp (**1c**, **2c**, and **3c**), no porphyrin-centered oxidation was observed, even at potentials up to 2.0 V. Complexes **3a**,**b** exhibit another reversible or quasi-reversible oxidation couple with $E_{1/2}$ = −0.11 and 0.28 V, respectively, and the corresponding oxidation couple for **3c** appears at $E_{1/2}$ = 0.59 V (Figure 7).

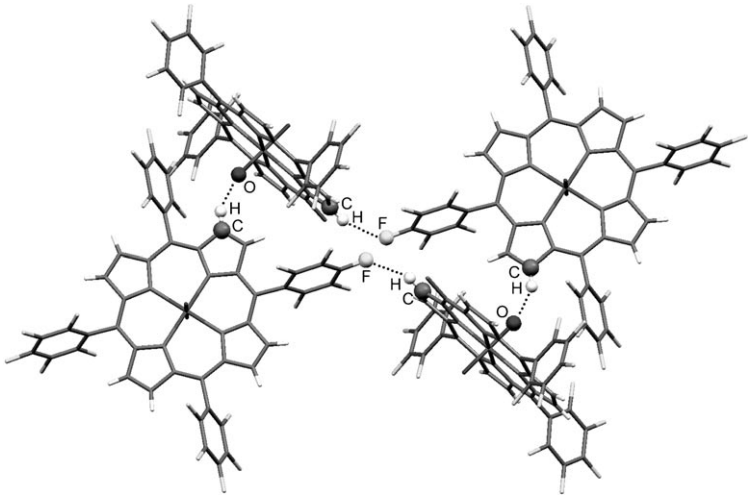

Figure 4. Interporphyrin C–H···O and C–H···F hydrogen bonding in **2b**·2MeOH. For clarity, the solvent molecules and some of the *meso*-pentafluorophenyl groups on the porphyrin rings are not shown.

The first reduction waves of **2a**–**g** are irreversible or quasi-reversible (Figure 6), with $E_{p,c}$ in the range of −0.70 to −1.15 V. These complexes have second reduction waves (quasi-reversible) at $E_{1/2} = -1.30$ to −1.72 V, which arise from the reduction of the porphyrin ring. An additional wave with $E_{p,a} = -0.25$ to −0.62 V, possibly resulting from oxidation of the decomposition products of reduced **2a**–**g**, is also present. For **3b**,**c**, the porphyrin-centered reduction occurs at $E_{1/2} = -1.83$ and −1.52 V, respectively.

Reactions of β-halogenated dioxoruthenium(VI) porphyrin complexes with hydrocarbons

Stoichiometric oxidation: Complexes **2b**,**c**,**e** are reactive toward hydrocarbon oxidation at room temperature, like previously reported β-hydrogenated counterparts **2a**,**d**,**f**, and other dioxoruthenium(VI) porphyrin complexes,[27] resulting in epoxidation of alkenes (such as styrenes and norbornene) and oxidation of benzylic C–H bonds (such as ethylbenzene and cumene). The yields of the oxidation products are listed in Table 5. In a typical reaction, a solution of the substrate (2 mmol) in degassed CH_2Cl_2 (3 mL) containing pyrazole (Hpz, 2% w/w) was treated with $[Ru^{VI}(por)O_2]$ (30 μmol) at room temperature, and the mixture was stirred for 8–24 h.

As shown in Table 5, styrene was oxidized to styrene oxide by **2b**,**c**,**e** in 74, 84, and 99% yields, respectively, and the oxidation of *para*-substituted styrenes by **2b**,**c** gave the epoxides in 60–84% yields (entries 1–5). *cis*-β-Methylstyrene was oxidized to its epoxide in 88% yield (*cis*-product) by **2c** and in 96% yield (*cis*:*trans* = 87:9) by **2e** (entry 6); *trans*-β-methylstyrene was oxidized to its epoxide in 56, 62, and 70% yield by **2b**,**c**,**e**, respectively (entry 7). Oxidation of cyclohexene by **2b**,**c**,**e** afforded cyclohexene epoxide in 35–41% yields, 2-cyclohexen-1-ol in 21–31% yields, and 2-cyclohexen-1-one in 10–15% yields (entry 8). Norbornene was oxidized by **2b**,**c**,**e** to its epoxide in 99% yield (entry 9).

Oxidation of C–H bonds by **2b**,**c**,**e** gave alcohols or ketones in 37–81% yields (entries 10–14, Table 5). Ethylbenzene was oxidized to *sec*-phenyl ethyl alcohol by **2b**,**c**,**e** in about 80% yield (entry 10); cumene was converted to acetophenone by **2b**,**c** in about 40% yield (entry 11). Oxidation of 9,10-dihydroanthracene (DHA), xanthene, and fluorene by **2b**,**c**,**e** gave anthrone, xanthone, fluorenone, respectively, in 40–46% yields (entries 12–14).

Kinetic studies: In 1,2-dichloroethane containing pyrazole (2% w/w), the time-dependent UV-visible spectra of the reaction mixtures generally exhibited clean isosbestic points,[44] similar to the reactions of other dioxoruthenium(VI) porphyrin complexes with alkenes.[27e,f,33c] Accordingly, all the kinetic measurements were performed in the presence of pyrazole.[45] Table 6 shows the second-order rate constants (k_2) for the reactions of **2a**–**f** with styrene, *para*-substituted styrenes *p*-X–C_6H_4CH=CH_2 (X = F, Cl, Me, MeO), *cis*- and *trans*-β-methylstyrene, cyclohexene, norbornene, ethylbenzene, cumene, xanthene, DHA, and fluorene.

Discussion

Effect of β-fluorination of porphyrin: Despite many studies on the effect of β-halogen substituents on the electronic properties and catalytic activities of metalloporphyrin complexes, a number of questions concerning the effect of β-fluorination still remain: 1) how the coordination of metal ion with an axial ligand is affected by β-fluorination, 2) how the β-fluorination of porphyrin affects the redox potential of metal center, and 3) whether β-fluorination of porphyrin could improve the reactivity of M=O moiety in oxometalloporphyrin complexes and, if yes, how large is the extent of rate acceleration arising from β-fluorination? These questions arise because halogenation of porphyrin ligands from tpp to 2,6-Cl_2tpp and F_{20}-tpp was found to increase the activities of ruthenium porphyrin oxidation catalysts, but **1c** was found to be a less effective catalyst than its F_{20}-tpp analogue (**1b**).[46] Moreover, although β-fluorination has been known to cause a large anodic shift in redox potentials of porphyrin rings,[20] few electrochemical studies have been reported on the change in redox potential of metal centers, especially in the case of oxometalloporphyrin complexes. To answer the questions, we examined the structures, spectral/electrochemical features, and reactivity of ruthenium porphyrin complexes bearing F_{28}-tpp ligand (**1c**, **2c**, and **3c**).

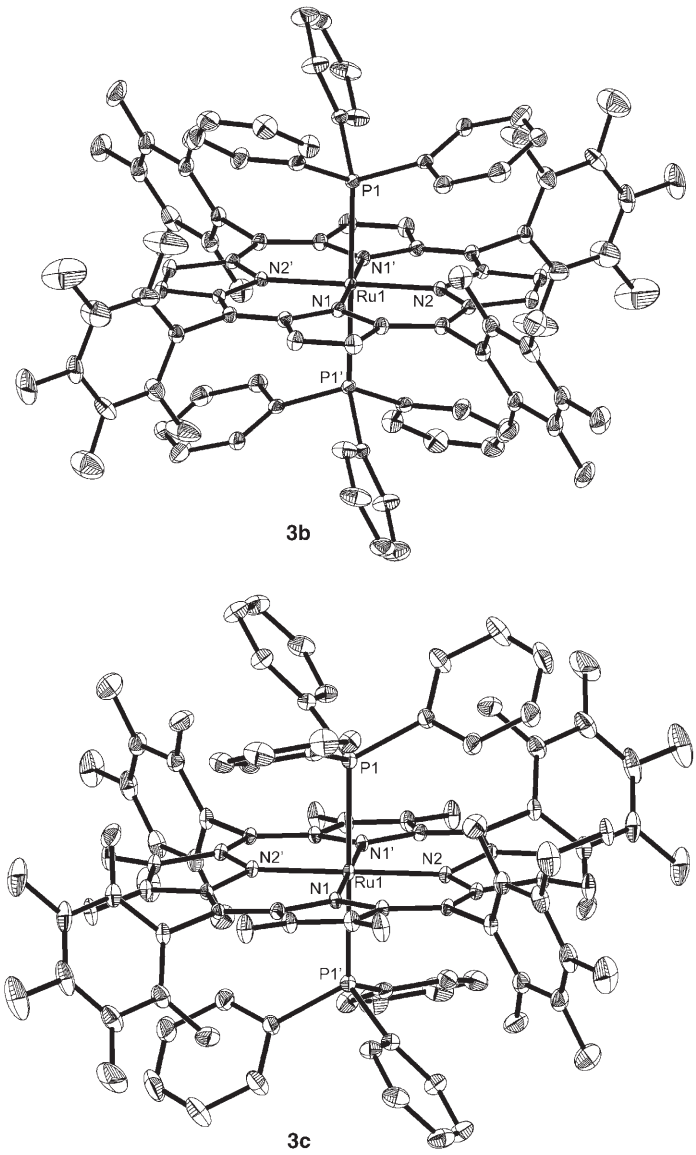

Figure 5. ORTEP drawings of **3b**,**c** with the atom-numbering scheme. Hydrogen atoms are not shown.

Table 3. Selected bond lengths [Å] and angles [°] for **3b**,**c**.

	3b	**3c**		**3b**	**3c**
Ru1−N1	2.050(2)	2.0458(18)	Ru1−N2	2.042(3)	2.0536(17)
Ru1−N1′	2.050(2)	2.0458(18)	Ru1−N2′	2.042(3)	2.0536(17)
Ru1−P1	2.4643(9)	2.4807(7)	Ru1−P1′	2.4643(9)	2.4807(7)
P1-Ru1-P1′	180.00(4)	180.00(2)	N1-Ru1-P1	92.26(8)	88.60(5)
N1-Ru1-P1′	87.74(8)	91.40(6)	N2-Ru1-P1	89.50(8)	91.19(5)
N2-Ru1-P1′	90.50(8)	88.81(5)	N1′-Ru1-P1	87.74(8)	91.40(6)
N1′-Ru1-P1′	92.26(8)	88.60(6)	N2′-Ru1-P1	90.50(8)	88.81(5)
N2′-Ru1-P1′	89.50(8)	91.19(5)	N1-Ru1-N2	89.63(10)	89.88(7)
N1-Ru1-N2′	90.37(10)	90.12(7)	N1′-Ru1-N1	180.00(6)	180.0
N1′-Ru1-N2	90.37(10)	90.12(7)	N1′-Ru1-N2′	89.63(10)	89.88(7)
N2-Ru1-N2′	180.00(15)	180.00(10)			

Crystal structures: Metal–axial-ligand distances in metalloporphyrin complexes are important structural parameters, which could affect the stability/reactivity of metal complexes. The unusual geometric parameters in **1b**·H_2O·2CH_2Cl_2 might stem from some extent of disorder of the related atoms (see the thermal ellipsoids in Figure 1). Therefore, a comparison between the Ru−C(CO) distances in **1b**·H_2O·2CH_2Cl_2 and **1c**·4H_2O·MeOH may not be useful. We compare the Ru−P bond lengths among **3b**,**c** and [Ru^{II}(oep)(PPh_3)$_2$],[43b] which are in the order F_{28}-tpp (2.481 Å) > F_{20}-tpp (2.464 Å) > oep (2.428 Å); this indicates that β-fluorination of F_{20}-tpp slightly lengthens the axial Ru−P bond.

As mentioned earlier, the porphyrin ring in **3c** exhibits a larger distortion than that in **3b**, implying the presence of additional steric congestion arising from the β-F atoms. The strong electron-withdrawing effect of the eight β-F substituents may also play a part. However, for both **1b**·H_2O·2CH_2Cl_2 and **1c**·4H_2O·MeOH, the porphyrin ring is essentially planar. The planar arrangement of the β-fluorinated porphyrin ring in **1c** is reminiscent of that in H_2(F_{28}-tpp),[47] [Zn(F_{20}-tpp)],[20] [Co^{II}(F_{28}-tpp)]·2Solv (Solv = toluene or THF),[36a] and [Rh^{III}(F_{28}-tpp)Me],[36b] but is in contrast to the significantly ruffled porphyrin ring in [Co^{III}(F_{28}-tpp)]Br[36c] and saddle-shaped porphyrin rings in [Pt^{II}(F_{28}-tpp)][36d] and β-chlorinated complex [Ru^{II}(β-Cl_8-F_{20}-tpp)(CO)]·H_2O·2 AcOEt.[34]

Spectroscopy: A comparison of the ^{1}H NMR chemical shifts of axial PPh_3 ligands between **3b**,**c** should reveal the change, caused by β-fluorination of the porphyrin ligand, in electron density of the metal ion and in the porphyrin ring current. Such chemical shifts of **3c** are larger than those of **3b**, indicating that the Ru^{II} ion in the former has a lower electron density and/or that the axial PPh_3 ligands in the former are less strongly affected by the porphyrin ring current (note the longer Ru−P bonds in **3c** than in **3b**). Complex **3b** has larger PPh_3 chemical shifts than [Ru^{II}(oep)(PPh_3)$_2$]; the observed trend of PPh_3 chemical shifts F_{28}-tpp > F_{20}-tpp > oep is in accord with the electron-withdrawing/donating capability of the porphyrin ligands and the Ru−P bond lengths in these complexes. Perfluorination of the β-H in **3b** to form **3c** increases the *o*-H chemical shifts of PPh_3 by 0.27 ppm, which is more than five times that (0.05 ppm) for perfluorination of the *meso*-phenyl groups of tpp in **3a** to form **3b**. This reflects different influence of the β-F substituents from that of the F substituents attached to the *meso*-phenyl groups.

Compared with **1b**/**2b**, the β-fluorinated complexes **1c**/**2c** have hypsochromically shifted UV-visible spectra. For example, the Soret bands are blue-shifted by ~12 nm on going from **1b**/**2b** to **1c**/**2c**. A similar phenomenon was observed for **3b** versus **3c**, with the Soret band of the latter being blue-shifted by 17 nm. However, β-bromination of **1d**/**2d** to **1e**/**2e** causes large bathochromic shifts in their UV-visible spec-

Table 4. Redox potentials (V versus $Cp_2Fe^{+/0}$) of ruthenium porphyrin complexes in CH_2Cl_2 at room temperature (electrolyte: 0.1 M $[nBu_4N]PF_6$).

	Oxidation		Reduction			
	I	II	I	II	III	other
	$E_{1/2}$	$E_{1/2}$	$E_{p,c}$ ($E_{1/2}$)	$E_{1/2}$	$E_{1/2}$	$E_{p,a}$
1c				−1.30	−1.79	
2a		0.60	−1.01 (−0.97)[a]	−1.72		−0.57
2b		1.25	−0.70 (−0.64)[a]	−1.30		−0.25
2c			−0.31[b]	−1.20[b]		
2d		0.71	−1.15[b]	−1.67		−0.60
2e		1.02	−0.86 (−0.76)[a]	−1.30		−0.35
2f		0.62	−1.11[b]	−1.65		−0.62
2g		0.70	−0.94[b]	−1.58		−0.49
3a	-0.11	0.78		−2.08[b]		
3b	0.28	1.33		−1.83		
3c	0.59			−1.52	−1.92	

[a] Quasi-reversible. [b] Irreversible, $E_{p,c}$.

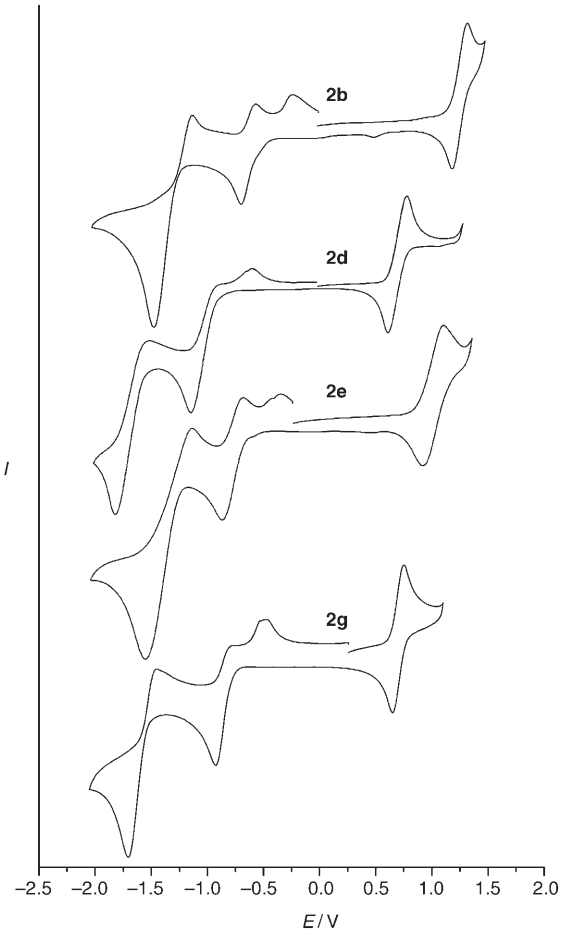

Figure 6. Cyclic voltammograms of **2b**,**d**,**e**,**g** (5×10^{-4} M) in CH_2Cl_2 containing 0.1 M $[nBu_4N]PF_6$. Scan rate: 50 mV s^{-1}.

tra. These observations are consistent with the previously reported hypsochromic shift for β-fluorination of $[Zn^{II}(tpp)]$[20,48] or $[Mn^{II}(F_{20}\text{-tpp})]$,[12b] and with the bathochromic shift for the β-bromination or -chlorination of **1b**.[34]

The higher ν(CO) frequency in the IR spectra of **1c** (1996 cm^{-1}) and **1e** (1954 cm^{-1}) than that of **1b** (1965 cm^{-1})

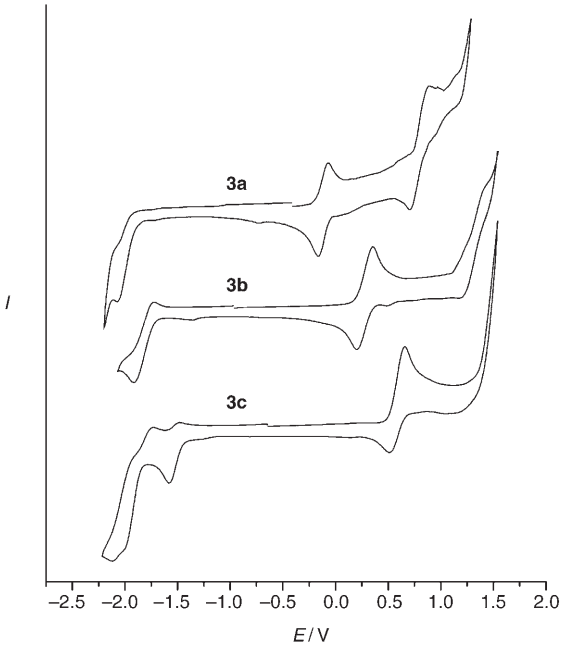

Figure 7. Cyclic voltammograms of **3a**–**c** (5×10^{-4} M) in CH_2Cl_2 containing 0.1 M $[nBu_4N]PF_6$. Scan rate: 50 mV s^{-1}.

Table 5. Stoichiometric oxidation of hydrocarbons by **2b**,**c**,**e** in CH_2Cl_2 containing pyazole (2% w/w).[a]

Entry	Substrate	Yield [%]		
		2b	**2c**	**2e**
1	styrene	74	84	99
2	4-fluorostyrene	84	80	
3	4-chlorostyrene	66	60	
4	4-methylstyrene	68	71	72
5	4-methoxystyrene	78	68	
6	*cis*-β-methylstyrene		88	96[b]
7	*trans*-β-methylstyrene	56	62	70
8	cyclohexene	35[c]	41[c]	40[c]
9	norbornene	99	99	99
10	ethylbenzene	78	81	78
11	cumene	42	37	
12	DHA[d]	44	46	
13	xanthene[d]	42	40	43
14	fluorene[d]	42	42	

[a] Yields were determined by GC using 1,4-dichlorobenzene as standard based on the amount of consumed $[Ru^{VI}(por)O_2]$. For entries 11–14, two equivalents of $[Ru^{VI}(por)O_2]$ was consumed for one equivalent of products. [b] *cis*-:*trans*-β-Methylstyrene epoxide = 87:9. [c] 2-Cyclohexen-1-ol (21, 24, and 31% yield for **2b**,**c**,**e**, respectively) and 2-cyclohexen-1-one (15, 11, and 10% yield for **2b**,**c**,**e**, respectively) were also obtained. [d] No radical coupling products were detected.

and **1d** (1940 cm^{-1}), respectively, implies a weaker $Ru^{II}\rightarrow$ CO back-bonding in the β-halogenated complexes, consistent with a decrease in electron density of the metal ion upon β-halogenation. The ν(RuO) frequencies of **2c**,**e** are not significantly different from those of **2b**,**d**. Complex **1c** has a higher ν(CO) frequency than $[Ru^{II}(\beta\text{-}Cl_8\text{-}F_{20}\text{-tpp})(CO)]$ (1990 cm^{-1}),[34] and, to our knowledge, is currently the carbonylruthenium(II) *meso*-tetraarylporphyrin with the highest ν(CO) frequency.[35]

Table 6. Second-order rate constants (k_2) for oxidation of alkenes by **2a–f** in 1,2-dichloroethane containing pyrazole (2% w/w) at 298 K.

Entry	Substrate	$k_2 \times 10^3$ [dm^{3}mol^{-1}s^{-1}]					
		2a	**2b**	**2c**	**2d**	**2e**	**2f**
1	styrene	3.8±0.3	14.0±0.8	158±8	2.2±0.2	13.2±0.7	2.2±0.1
2	4-fluorostyrene		14.9±0.8	182±9		13.8±0.7	2.6±0.1
3	4-chlorostyrene	11.4±0.4[a]	16.8±0.9	210±10			
4	4-methylstyrene	8.81±0.2[a]	24±1	530±30			
5	4-methoxystyrene	47.4±2.5[a]	60±3	1200±60			
6	*cis*-β-methylstyrene		8.6±0.5	240±10		19.2±0.9	5.6±0.3
7	*trans*-β-methylstyrene		14.4±0.7	193±9		4.7±0.3	2.9±0.1
8	cyclohexene	4.0±0.2	41±2	620±30	21±1	32±2	
9	norbornene	3.01±0.09[a]	42±2	207±9	2.8±0.2		
10	ethylbenzene	0.52±0.03	3.1±0.2	26±1	0.36±0.02	1.24±0.07	0.77±0.04
11	cumene			16.6±0.9	0.40±0.02		
12	xanthene		3800±200	59000±3000	450±20		
13	DHA		1740±80	22500±900	170±9		
14	fluorene		94±5	1320±60	58±3		

[a] From reference [27c].

Electrochemical properties: The first reduction waves of **2a–g** occur at potentials substantially more anodic than the reduction of the corresponding porphyrin ligands and are assigned to the reduction of Ru^{VI} to Ru^{V}. Since this reduction is irreversible for **2c**,**d**,**f**,**g**, only the $E_{p,c}$ values can be compared among all the complexes. From Table 4, one can see that the $E_{p,c}(Ru^{VI/V})$ values of **2a–g** are in the order: tmp, D_4-por* < tpp, ttp < β-Br_8-tmp < F_{20}-tpp < F_{28}-tpp, that is, they essentially increase with the electron-withdrawing capability of peripheral substituents of the porphyin ligands.

The $E_{p,c}(Ru^{VI/V})$ of **2c** is 390 mV more anodic than that of **2b**, and on going from **2d** to **2e**, an increase of $E_{p,c}(Ru^{VI/V})$ by 290 mV was observed. Remarkably, perfluorination of tpp to F_{28}-tpp (**2a**→**2c**) increases the $E_{p,c}(Ru^{VI/V})$ by 700 mV.

For **3a–c**, the oxidation couples at $E_{1/2} = -0.11$ (**3a**), 0.28 (**3b**), and 0.59 V (**3c**) have potentials substantially less anodic than those of the corresponding porphyrin-centered oxidations; we attribute these couples to the oxidation of Ru^{II} to Ru^{III}. The $E_{1/2}(Ru^{III/II})$ values of **3a–c** are in the order tpp < F_{20}-tpp < F_{28}-tpp, consistent with the electron-withdrawing capability of the porphyrin substituents. The β-fluorination of **3b** to **3c** increases the $E_{1/2}(Ru^{III/II})$ by 310 mV. Perfluorination of tpp to F_{28}-tpp in the case of **3a**→**3c** results in an increase of $E_{1/2}(Ru^{III/II})$ by 700 mV, the same as that of the metal-centered reduction of Ru^{VI} to Ru^{V} in $[Ru^{VI}(por)O_2]$ (**2a**→**2c**).

β-*Halogenation-induced rate acceleration*: It has been well established that the effect of β-halogen substituents of *meso*-tetraarylporphyrins stems from the electron-withdrawing capability of halogens and in the cases of chlorine and bromine from saddle distortion of the porphyrin ring as well.[21] Provided that the metalloporphyrin-catalyzed hydrocarbon oxidations proceed through an oxometalloporphyrin reactive intermediate, it can be expected, qualitatively, that β-halogenation will make the reactive intermediate more electrophilic by reducing the electron density of the porphyrin ring, thus promoting its reactivity toward hydrocarbons. However, the extent of rate acceleration arising from β-halogenation is hard to predict. The k_2 values determined in this work first provide a quantitative measure of the β-halogenation-induced rate acceleration of hydrocarbon oxidations by an oxometalloporphyrin.

Inspection of the data in Table 6 reveals that **2c** reacts with styrene, 4-fluorostyrene, 4-chlorostyrene, and *trans*-β-methylstyrene about 12 times faster than **2b** (entries 1–3 and 7). For 4-methylstyrene and 4-methoxystyrene, the β-fluorination-induced rate acceleration is considerably larger (k_2(**2c**)/k_2(**2b**) ≈ 20, entries 4 and 5). The largest rate acceleration was observed for *cis*-β-methylstyrene, whose reaction with **2c** is about 28 times faster than with **2b** (entry 6). In the cases of cyclohexene and norbornene, the k_2(**2c**)/k_2(**2b**) ≈ 15 and 5, respectively (entries 8 and 9). The C–H bond oxidation of ethylbenzene by **2b**,**c**, which is slower than the alkene epoxidation, again exhibits a significant β-fluorination-induced rate acceleration: k_2(**2c**)/k_2(**2b**) ≈ 8 (entry 10). The C–H bond oxidations of DHA, xanthene, and fluorene by **2b**,**c** are much faster than the alkene epoxidation, with k_2 values of up to 59±3 (entries 12–14). In these cases, the β-fluorination-induced rate acceleration k_2(**2c**)/k_2(**2b**) ≈ 13–16.

The β-bromination of **2d** to **2e** results in a rate acceleration with k_2(**2e**)/k_2(**2d**) ≈ 6 for styrene and 3 for ethylbenzene (entries 1 and 10 in Table 6), about half that found for the β-fluorination of **2b** to **2c**. This might arise from the smaller electron-withdrawing capability of bromo than fluoro groups.

Perfluorination of the *meso*-phenyl groups in **2a** to form **2b** leads to <4-fold increase in k_2 for styrene epoxidation (entry 1 in Table 6). For the oxidation of ethylbenzene, the k_2(**2b**)/k_2(**2a**) value ≈ 6 (entry 10 in Table 6).

It was reported that perfluorination of H_2(tpp) to H_2(F_{28}-tpp) increases the lowest IP of the porphyrin by up to 1.65 eV.[22b,c] From the data in Table 6, one can assess the effect of perfluorination of **2a** on its reactivity toward hydrocarbons. For example, the reacions of **2c** with styrene, cyclohexene, and ethylbenzene are about 42, 155, and 50 times faster, respectively, than those of **2a** (entries 1, 8, and 10 in Table 6).

Dual-parameter Hammett correlation: Our previous work[27f] demonstrated that the oxidation of styrenes *p*-X–$C_6H_4CH{=}CH_2$ (X = H, F, Cl, Me, MeO) by $[Ru^{VI}(por)O_2]$ (in which por = β-Ph_8-tpp, 2,6-Cl_2tpp, and 2,4,6-$(MeO)_3$tpp) exhibits a linear $\log k_{rel}$ versus (σ_{mb}, $\sigma^{\cdot}_{JJ}$) plot, whereby k_{rel} = k_2(X)/k_2(H), $\sigma^{\cdot}_{JJ}$ is a radical parameter,[49] with ρ_{mb} ranging

from −0.58 to −0.77 and $\rho_{JJ}^{\cdot}$ from 1.01 to 1.67 ($|\rho_{JJ}^{\cdot}/\rho_{mb}|$ = 1.63–2.17). This is compatible with the rate-limiting formation of a carboradical intermediate. From the data in Table 6 (entries 1–5), we obtain similar dual-parameter Hammett correlation for the oxidation of styrenes by **2c**: $\log k_{rel} = -0.82\sigma_{mb} + 1.39\sigma_{JJ}^{\cdot}$ ($|\rho_{JJ}^{\cdot}/\rho_{mb}| = 1.69$). The positive $\rho_{JJ}^{\cdot}$ values suggest that the epoxidation reaction is promoted by delocalizing spin density at the radical center; the negative ρ_{mb} values are consistent with the electrophilic nature of the dioxoruthenium(VI) complexes. In all cases, the magnitude of $|\rho_{JJ}^{\cdot}/\rho_{mb}|$ (>1) suggests that the spin delocalization effect is more important than the polar substituent effect. These observations reveal that alkene epoxidations by β-hydrogenated and β-fluorinated dioxoruthenuim(VI) porphyrin complexes proceed by similar mechanism.

Effect of thermodynamic driving force on reaction rate constants

Relationship between second-order rate constants k_2 and reduction potentials of Ru^{VI} to Ru^{V}: In a prvious study on the oxidation of various alkenes by **2a**, a linear correlation between $\log k_2$ and $E_{1/2}$ of one-electron oxidation of alkenes, with a slope of $-1.1\ V^{-1}$, was observed,[27c] indicating that little charge transfer is involved in the transition state. The correlation between $\log k_2$ and reduction potentials of dioxoruthenium(VI) porphyrin complexes (Ru^{VI} to Ru^{V}) has not been reported in the literature. Such a correlation is important to the design of efficient ruthenium porphyrin catalysts for hydrocarbon oxidation through tuning structural and electronic properties.

As shown in Tables 4 and 6, the k_2 for the oxidation of styrene or ethylbenzene by **2a–f** increases with the ease of Ru^{VI} to Ru^{V} reduction. Plotting $\log k_2$ against the $E_{p,c}(Ru^{VI/V})$ of **2a–f** for their reactions with styrene and ethylbenzene results in a good linearity (Figure 8), with slopes of $2.2\ V^{-1}$ (styrene) and $2.1\ V^{-1}$ (ethylbenzene). The slopes of these plots are substantially smaller than that ($9.1\ V^{-1}$) for the oxidation of styrene by $[Cr^{V}(por)(O)(X)]$ reported by Bruice and co-workers.[24d] This suggests that the extent of charge transfer in the rate-determining step is smaller for the hydrocarbon oxidation by $[Ru^{VI}(por)O_2]$ than by $[Cr^{V}(por)(O)(X)]$.

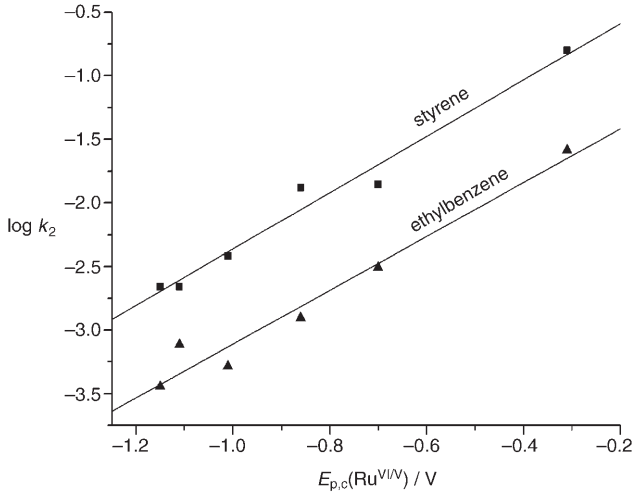

Figure 8. Plots of $\log k_2$ versus $E_{p,c}(Ru^{VI/V})$ for the oxidation of styrene and ethylbenzene by different dioxoruthenium(VI) porphyrin complexes **2a–f**.

Correlation of rate constants and bond dissociation energies (BDEs): Hydrogen-atom abstraction from a C–H bond is an important pathway in the oxidation of C–H bonds of benzylic and allylic substrates by metal–oxo complexes. Meyer and co-workers proposed a hydrogen-atom abstraction mechanism for oxidation of C–H bonds by *cis*-$[(bpy)_2(py)Ru^{IV}O]^{2+}$;[50] We suggested a hydrogen-atom abstraction mechanism for C–H bond oxidation by $[Ru^{VI}(por)O_2]$.[27c] Recently, Mayer and co-workers demonstrated a clear linear correlation between $\log k'$ (k' is the k_2 divided by the number of reactive C–H bonds) and BDEs for C–H bond oxidation by $[(bpy)_2(py)Ru^{IV}O]^{2+}$ involving a hydrogen-atom abstraction mechanism.[29] A similar linear correlation has been observed for hydrocarbon oxidation by permanganate,[51] $[Fe^{IV}(O)(N_4py)]^{2+}$ (N_4py = *N*,*N*-bis(2-pyridylmethyl)-bis(2-pyridyl)methylamine),[52] and $[Fe^{IV}(O)(Bn\text{-}tpen)]^{2+}$ (Bn-tpen = *N*-benzyl-*N*,*N*′,*N*′-tris(2-pyridylmethyl)-1,2-diaminoethane).[52]

In this work, we examined $\log k'$ versus BDE plots for the C–H bond oxidations by **2b–d**; the plots for **2c**,**d** are shown in Figure 9. These plots all exhibit a good linearity, with slopes of −0.28 (**2b**), −0.31 (**2c**), and −0.28 (**2d**). From the previously reported linear $\log k'$ versus BDE plots for the reaction of hydrocarbons with metal–oxo complexes, the slopes were found to be −0.55 for permanganate,[51] −0.36 for $[(bpy)_2(py)Ru^{IV}O]^{2+}$,[29] and −0.19 for $[Fe^{IV}(O)(N_4py)]^{2+}$ and $[Fe^{IV}(O)(Bn\text{-}tpen)]^{2+}$.[52] Apparently, the hydrocarbon oxidation by dioxoruthenium(VI) porphyrin complexes is less sensitive to changes in BDE than by permanganate and $[(bpy)_2(py)Ru^{IV}O]^{2+}$, but more sensitive to changes in BDE than by the cationic Fe^{IV}–oxo complexes. These oxidants are previously proposed to oxidize C–H bonds by menas of a hydrogen-atom abstraction mechanism. The lessened sensitivities of the porphyrin systems relative to the permanganate and $[(bpy)_2(py)Ru^{IV}O]^{2+}$ systems may result from more profound changes in the coordination sphere and solvation in these last two systems that occur during the hydrogen-atom abstraction processes. Possibly, the structural and electronic reorganization of ruthenium porphyrin lags behind the hydrogen-atom transfer in the rate-determining step; such imperfect synchronicity could reduce the dependence of the rate on the substrate BDE in a manner analogous to that proposed in proton transfer. Future studies on the hydrogen-atom and electron self-exchange reactions of the relevant dioxoruthenium(VI) porphyrin complexes may provide insight into the mechanisms. In view of the good correlation of k_2 with substrate BDEs, we conclude that the reaction mechanism is a hydrogen-atom abstraction from the substrate by dioxoruthenium(VI) porphyrin complexes.

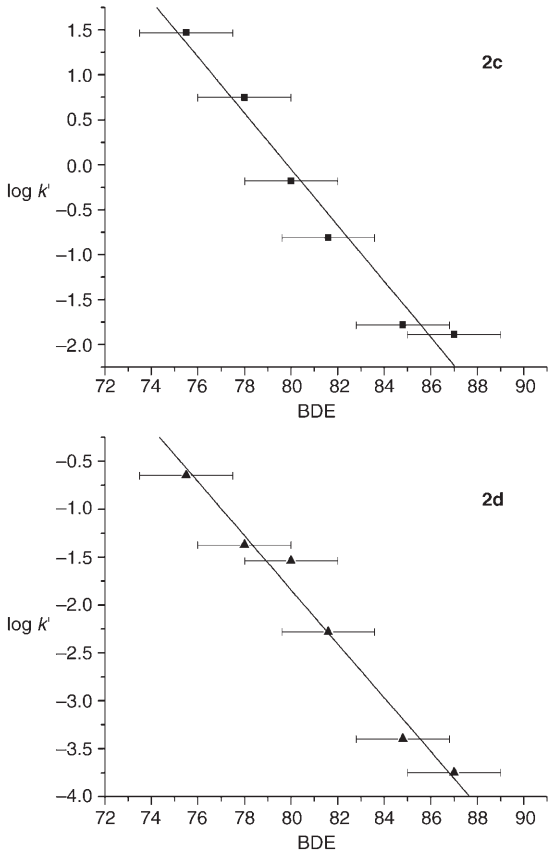

Figure 9. Plots of $\log k'$ versus BDE for C–H bond oxidations of xanthene, DHA, fluorene, cyclohexene, cumene, and ethylbenzene by **2c**,**d**. The BDE values are taken from reference [29].

Conclusion

The following conclusions can be drawn from the present work:

1) Reactive β-halogenated oxometalloporphyrin complexes, $[Ru^{VI}(por)O_2]$ (por = F_{28}-tpp, β-Br_8-tmp) can be isolated as a spectroscopically pure solid from oxidation of their carbonylruthenium(II) porphyrin precursors with *m*-CPBA. The crystal structure of a dioxoruthenium(VI) complex bearing a sterically unencumbered porphyrin ligand has been determined by X-ray crystallography.
2) The crystal structures and/or spectroscopic properties of $[Ru^{II}(F_{28}\text{-tpp})(CO)]$, $[Ru^{VI}(F_{28}\text{-tpp})(PPh_3)_2]$, and $[Ru^{VI}(F_{28}\text{-tpp})O_2]$, when compared with those of their β-hydrogenated counterparts, show that β-fluorination considerably affects metal–axial-ligand coordination, porphyrin ring current, and redox behavior of the ruthenium ion.
3) The second-order rate constants k_2 of reactions between β-halogenated dioxoruthenium(VI) porphyrin complexes and hydrocarbons markedly depend on the nature of the porphyrin ligands and the hydrocarbons. Remarkable β-halogenation-induced rate acceleration is observed on going from F_{20}-tpp to F_{28}-tpp for oxidation of styrenes, cyclohexene, DHA, xanthene, and fluorene. Perfluorination of the tpp in $[Ru^{VI}(tpp)O_2]$ results in up to 155-fold increase in k_2 for its hydrocarbon oxidation reactions.
4) A linear dual-parameter Hammett correlation [$\log k_{rel}$ versus (σ_{mb}, $\sigma_{JJ}^{\cdot}$) plot] shows that, for the dioxoruthenium(VI)-mediated alkene epoxidation, β-fluorination does not alter the reaction mechanism.
5) The rate constants k_2 show a moderate dependence on the reduction potentials of Ru^{VI} to Ru^{V}.
6) There is a linear correlation between the log of the rate constants and the BDEs of C–H bonds, providing a strong evidence for hydrogen-atom abstraction mechanism in oxidation of hydrocarbons by dioxoruthenium(VI) porphyrin complexes.

Experimental Section

General: $Ru_3(CO)_{12}$ (Strem), *m*-CPBA (55%, Merck), pyrazole (98%, Aldrich), and $H_2(F_{20}$-tpp) (synthetic, Aldrich), together with the solvents (AR grade) for synthetic studies, were used as received unless otherwise specified. The solvent 1,2-dichloroethane for kinetic studies was refluxed over calcium chloride followed by distillation. All alkene substrates except *cis*-β-methylstyrene were purchased from commercial vendors and purified by either vacuum distillation from calcium hydride or by being passed through a dry column of activated alumina (Grade I). *cis*-β-Methylstyrene,[53] $H_2(D_4$-por*),[54] $H_2(F_{28}$-tpp),[20] H_2(β-Br_8-tmp),[9] $[Ru^{II}(por)(CO)]$ (por = tpp **1a**,[30e] tmp **1d**,[32b] D_4-por* **1f**[33a,c]), and $[Ru^{VI}(por)O_2]$ (por = tpp **2a**,[27b,c] tmp **2d**,[32b] D_4-por* **2f**[33c]) were prepared by literature methods. UV-visible spectra were measured on a Perkin–Elmer Lambda 19 or a Hewlett-Packard 8453 diode array spectrophotometer. IR spectra were recorded on a Nicolet 20 FXC FT-IR spectrometer (KBr pellets). NMR spectra were acquired on a Bruker DPX-300 spectrometer. FAB mass spectra were obtained on a Finnigan MAT 95 mass spectrometer with 3-nitrobenzyl alcohol as the matrix, whereas electrospray mass spectra (ES MS) on a Finnigan LCQ quadrupole ion trap mass spectrometer. Cyclic voltammograms were measured on a Princeton Applied Research Model 273 A potentiostat/galvanostat coulometer and Model 270/250 universal programmer using a three-electrode cell system (working electrode: glassy carbon, counter electrode: platinum wire, reference electrode: 0.1 M $Ag/AgNO_3$ in MeCN) with ferrocene as an internal standard.

Preparation of carbonylruthenium(II) porphyrin complexes 1b,c,e: A mixture of $[Ru_3(CO)_{12}]$ (100 mg) and H_2(por) (100 mg) in freshly distilled 1,2,4-trichlorobenzene (50 mL) was refluxed overnight under argon. The solvent of the mixture was then removed by distillation and the residue obtained was subjected to column chromatography on alumina. Upon removal of unreacted H_2(por) and some impurities with CH_2Cl_2/hexane (1:1 v/v) as eluent, the brick red band containing the desired product was eluted with CH_2Cl_2/acetone (1:1 v/v).

$[Ru^{II}(F_{20}$-tpp)(CO)] (1b): Yield: 93%; ^{19}F NMR ($CDCl_3$): $\delta = -137.5$ (d, $J = 24$ Hz, 4F; *o*-F), −139.2 (d, $J = 24$ Hz, 4F; *o*′-F), −152.0 (t, $J = 19$ Hz, 4F; *p*-F), −158.4 (dd, $J = 15$ Hz, 4F; *m*-F), −159.1 ppm (d, $J = 15$ Hz, 4F; *m*′-F); FAB-MS: *m*/*z*: 1102 [M^+], 1074 [M^+−CO]. The ^{1}H NMR, IR, and UV-visible spectra data are identical to those of the same complex prepared previously in 55% yield from the reaction of $[Ru_3(CO)_{12}]$ and $H_2(F_{20}$-tpp) in refluxing *o*-dichlorobenzene.[31b]

$[Ru^{II}(F_{28}$-tpp)(CO)] (1c): Yield: 38%; ^{19}F NMR ($CDCl_3$): $\delta = -138.1$ (d, $J = 25$ Hz, 4F; *o*-F), −140.3 (d, $J = 24$ Hz, 4F; *o*′-F), −144.6 (s, 8F; β-F), −149.9 (t, $J = 20$ Hz, 4F; *p*-F), −161.5 (d, $J = 16$ Hz, 4F; *m*-F), −162.2 ppm (d, $J = 16$ Hz, 4F; *m*′-F); IR (KBr): $\tilde{\nu} = 1996$ cm^{-1} (CO); UV/Vis (CH_2Cl_2): λ_{max} ($\log \varepsilon$) = 394 (5.56), 516 nm (4.32); FAB-MS: *m*/*z* 1246 [M^+], 1218 [M^+−CO].

[Ru^{II}(β-Br$_8$-tmp)(CO)] (1e): Yield: 96%; ^{1}H NMR ($CDCl_3$): $\delta = 7.18$ (br, 8H; *m*-H), 2.58 (s, 12H; *p*-Me), 1.94 (s, 12H; *o*-Me), 1.70 ppm (s, 12H; *o*′-Me); IR (KBr): $\tilde{\nu} = 1954\ cm^{-1}$ (CO); UV/Vis (CH_2Cl_2): λ_{max} ($\log\varepsilon$) = 430 (5.50), 560 nm (4.41); FAB-MS: *m*/*z* 1541 [M^+], 1513 [M^+−CO].

Preparation of dioxoruthenium(VI) porphyrin complexes 2b,c,e: These complexes were prepared from treatment of **1b**,**c**,**e** with *m*-CPBA in CH_2Cl_2 at room temperature according to the procedure reported for the preparation of **2f**.[33c]

[Ru^{VI}(F$_{20}$-tpp)O$_2$] (2b): Yield: 90%; ^{1}H NMR ($CDCl_3$): $\delta = 9.18$ ppm (s, 8H; β-H); ^{19}F NMR ($CDCl_3$): $\delta = -136.8$ (dd, $J = 21$, 6 Hz, 8F; *o*-F), −149.2 (t, $J = 21$ Hz, 4F; *p*-F), −161.2 ppm (dd, $J = 23$, 7 Hz, 8F; *m*-F); IR (KBr): $\tilde{\nu} = 826\ cm^{-1}$ (RuO); UV/Vis (CH_2Cl_2): λ_{max} ($\log\varepsilon$) = 412 (5.34), 506 nm (4.42); FAB-MS: *m*/*z* 1106 [M^+], 1090 [M^+−O], 1074 [M^+−2O].

[Ru^{VI}(F$_{28}$-tpp)O$_2$] (2c): Yield: 30%; ^{19}F NMR ($CDCl_3$): $\delta = -137.2$ (dd, $J = 22$, 7 Hz, 8F; *o*-F), −143.3 (s, 8F; β-F), −148.9 (t, $J = 21$ Hz, 4F; *p*-F), −160.9 ppm (dd, $J = 23$, 7 Hz, 8F; *m*-F); IR (KBr): $\tilde{\nu} = 823\ cm^{-1}$ (RuO); UV/Vis (CH_2Cl_2): λ_{max} ($\log\varepsilon$) = 399 (5.35), 494 nm (4.46); ES-MS: *m*/*z* 1250 [M^+], 1234 [M^+−O], 1218 [M^+−2O].

[Ru^{VI}(β-Br$_8$-tmp)O$_2$] (2e): Yield: 80%; ^{1}H NMR ($CDCl_3$): $\delta = 7.20$ (s, 8H; *m*-H), 2.62 (s, 12H; *p*-Me), 1.97 ppm (s, 24H; *o*-Me); IR (KBr): $\tilde{\nu} = 824\ cm^{-1}$ (RuO); UV/Vis (CH_2Cl_2): λ_{max} ($\log\varepsilon$) = 456 (5.32), 540 nm (4.34); ES-MS: *m*/*z* 1545 [M^+], 1529 [M^+−O], 1513 [M^+−2O].

Preparation of bis(triphenylphosphane)ruthenium(II) porphyrin complexes 3b,c: A mixture of **2b** or **2c** (100 mg) and PPh_3 (100 mg) in CH_2Cl_2 (10 mL) was stirred for 1 h. The solvent of the mixture was then removed by distillation and the residue was washed with ethanol.

[Ru^{II}(F$_{20}$-tpp)(PPh$_3$)$_2$] (3b): Yield: 78%; ^{1}H NMR ($CDCl_3$): $\delta = 8.08$ (s, 8H; β-H), 6.77 (t, $J = 7.1$ Hz, 6H; *p*-H), 6.47 (t, $J = 7.0$ Hz, 12H; *m*-H), 4.30 ppm (br, 12H; *o*-H); ^{19}F NMR ($CDCl_3$): $\delta = -135.4$ (d, $J = 19$ Hz, 8F; *o*-F), −153.7 (t, $J = 20$ Hz, 4F; *p*-F), −162.6 (t, $J = 19$ Hz, 8F; *m*-F); ^{31}P NMR ($CDCl_3$): $\delta = 5.61$; UV/Vis (CH_2Cl_2): λ_{max} ($\log\varepsilon$) = 413 (5.34), 506 (4.12), 532 nm (4.17); FAB-MS: *m*/*z* 1336 [M^+−PPh_3], 1074 [M^+−2PPh_3].

[Ru^{II}(F$_{28}$-tpp)(PPh$_3$)$_2$] (3c): Yield: 80%; ^{1}H NMR ($CDCl_3$): $\delta = 6.95$ (t, $J = 7.3$ Hz, 6H; *p*-H), 6.66 (t, $J = 7.0$ Hz, 12H; *m*-H), 4.57 ppm (br, 12H; *o*-H); ^{19}F NMR ($CDCl_3$): $\delta = -138.4$ (d, $J = 19$ Hz, 8F; *o*-F), −145.3 (s, 8F; β-F), −152.3 (t, $J = 21$ Hz, 4F; *p*-F), −162.9 ppm (t, $J = 19$ Hz, 8F; *m*-F); ^{31}P NMR ($CDCl_3$): $\delta = 4.59$; UV/Vis (CH_2Cl_2): λ_{max} ($\log\varepsilon$) = 396 (5.51), 498 (4.06), 518 nm (4.16); FAB-MS: *m*/*z* 1480 [M^+−PPh_3], 1218 [M^+−2PPh_3].

Kinetic studies: A solution of dioxoruthenium(VI) porphyrin in 1,2-dichloroethane containing pyrazole (2% w/w) was treated with at least 100-fold excess of hydrocarbon substrate at 298 ± 0.2 K. The absorbance (*A*) of the Soret band in the UV-visible spectrum of the reaction mixture at different reaction time (*t*) was measured, by using standard 1.0 cm quartz cuvettes, on a Hewlett–Packard 8453 diode array spectrophotometer interfaced with an IBM-compatible PC and equipped with a Lauda RM6 circulating water bath. A nonlinear least-squares fitting of the (A_f−A_t) versus *t* data over four half-lives ($t_{1/2}$) by the equation (A_t−A_t) = (A_f−A_i)exp(−$k_{obs}t$) (in which A_f and A_i are the final and initial absorbance, respectively, and A_t is the absorbance measured at time *t*) gave the pseudo-first-order rate constant k_{obs} of the reaction. Upon determination of the k_{obs} values at various concentrations of the hydrocarbon substrate, the second-order rate constant k_2 of the reaction was obtained from the linear least-squares fitting of the k_{obs} versus hydrocarbon concentration plot. No rate saturation was observed over the hydrocarbon concentrations employed in this work.

X-ray crystal structure determinations: Details of the data collection and refinement are given in Table 7. Single crystals of **1b**·H_2O·2CH_2Cl_2 (0.30 × 0.28 × 0.20 mm^3), **1c**·4H_2O·MeOH (0.18 × 0.10 × 0.08 mm^3), **2b**·2MeOH (0.40 × 0.40 × 0.10 mm^3), **3b** (0.50 × 0.50 × 0.16 mm^3), and **3c** (0.40 × 0.3 × 0.28 mm^3) were obtained from slow evaporation of a solution of **1b** in CH_2Cl_2, **1c** or **2b** in CH_2Cl_2/MeOH, and **2b** or **3b** in CH_2Cl_2/hexane (the solutions were kept open to air, except for **2b**). The data were collected at 294(2) K using graphite-monochromatized $Mo_{K\alpha}$ radiation ($\lambda = 0.71073$ Å) on a Siemens P4 diffractometer for **1b**·H_2O·2CH_2Cl_2, a Bruker SMART CCD diffractometer for **1c**·4H_2O·MeOH and **3b**,**c**, and a MAR diffractometer for **2b**·2MeOH. The structure was solved by employing the SHELXS-97 program and refined by full-matrix least-squares on F^2 by using the SHELXL-97 program. In the case of **1b**·H_2O·2CH_2Cl_2, although the unit cell parameters feature $a = b$ and $\alpha = \beta = \gamma = 90°$, this crystal actually belongs to the triclinic rather than the orthorhombic system because the C_4 axis in which

Table 7. Crystal data and structure refinement for **1b**·H_2O·2CH_2Cl_2, **1c**·4H_2O·MeOH, **2b**·2MeOH, **3b**, and **3c**.

	1b·H_2O·2CH_2Cl_2	**1c**·4H_2O·MeOH	**2b**·2MeOH	**3b**	**3c**
formula	$C_{45}H_8F_{20}N_4ORu$· H_2O·2CH_2Cl_2	$C_{45}F_{28}N_4ORu$· 4H_2O·CH_3OH	$C_{44}H_8F_{20}N_4O_2Ru$· 2CH_3OH	$C_{80}H_{38}F_{20}N_4P_2Ru$	$C_{80}H_{30}F_{28}N_4P_2Ru$
M_r	1289.49	1349.67	1169.70	1598.15	1742.12
cryst system	triclinic	triclinic	monoclinic	monoclinic	monoclinic
space group	$P\bar{1}$	$P\bar{1}$	$P2_1/c$	$C2/c$	$P2_1/c$
a [Å]	18.370(4)	11.313(3)	14.459(3)	28.303(4)	13.2730(14)
b [Å]	18.370(4)	11.636(3)	13.075(3)	13.2645(16)	13.4090(15)
c [Å]	8.168(2)	19.331(5)	12.285(3)	19.608(4)	19.844(2)
α [°]	90.00(3)	93.160(5)	90.00(3)	90.00	90.00
β [°]	90.00(3)	100.216(6)	113.85(3)	117.340(5)	109.251(2)
γ [°]	90.00(3)	103.628(6)	90.00(3)	90.00	90.00
V [Å^3]	2756(1)	2421(1)	2124.2(7)	6539.2(17)	3334.2(6)
Z	2	2	2	4	2
F(000)	1264	1320	1152	3200	1410
ρ_{calcd} [Mg m^{-3}]	1.554	1.851	1.829	1.623	1.433
μ [mm^{-1}]	0.586	0.487	0.510	0.398	0.398
index ranges	$0 \le h \le 21$	$-14 \le h \le 13$	$-17 \le h \le 10$	$-36 \le h \le 34$	$-17 \le h \le 11$
	$-22 \le k \le 22$	$-15 \le k \le 14$	$-15 \le k \le 15$	$-17 \le k \le 16$	$-16 \le k \le 17$
	$-9 \le l \le 9$	$-25 \le l \le 18$	$-14 \le l \le 14$	$-25 \le l \le 24$	$-25 \le l \le 25$
reflns collected	5861	16220	8727	21670	22508
independent reflns	5754	10938	3826	7525	7683
data/restraints/parameters	5754/32/768	10938/0/742	3826/4/340	7525/75/473	7683/0/520
final *R* indices [$I > 2\sigma(I)$]	$R1 = 0.089$	$R1 = 0.075$	$R1 = 0.041$	$R1 = 0.060$	$R1 = 0.052$
	w$R2 = 0.159$	w$R2 = 0.170$	w$R2 = 0.122$	w$R2 = 0.191$	w$R2 = 0.138$
goodness-of-fit on F^2	1.215	0.771	1.071	1.046	1.077
largest diff peak/hole [e Å^{-3}]	0.990/−0.913	0.913/−0.643	1.137/−0.511	0.951/−0.879	0.599/−0.651

the ruthenium atom is situated does not pass through all the atoms of the axial H_2O-Ru-C-O moiety.

CCDC-278038 (**1b**·H_2O·$2CH_2Cl_2$), −278039 (**1c**·$4H_2O$·MeOH), −278040 (**2b**·2MeOH), −278041 (**3b**), and −278042 (**3c**) contains the supplementary crystallographic data for this paper. These data can be obtained free of charge from The Cambridge Crystallographic Data Centre via www.ccdc.cam.ac.uk/data_request/cif.

Acknowledgements

This work was supported by the University Development Fund of The University of Hong Kong, the Hong Kong Research Grants Council (HKU 7384/02P), and the University Grants Committee of the Hong Kong SAR of China (Area of Excellence Scheme, AoE/P-10/01).

[1] Abbreviations for the porphyrin ligands: tpp = 5,10,15,20-tetraphenylporphyrinato(2−), ttp = 5,10,15,20-tetrakis(*p*-tolyl)porphyrinato(2−), tmp = 5,10,15,20-tetrakis(2,4,6-trimethylphenyl)porphyrinato(2−), D_4-por* = 5,10,15,20-tetrakis[(1*S*,4*R*,5*R*,8*S*)-1,2,3,4,5,6,7,8-octahydro-1,4:5,8-dimethanoanthracen-9-yl]porphyrinato(2−), 2,6-Cl_2tpp = 5,10,15,20-tetrakis(2,6-dichlorophenyl)porphyrinato(2−), F_{20}-tpp = 5,10,15,20-tetrakis(pentafluorophenyl)porphyrinato(2−), F_{28}-tpp = 2,3,7,8,12,13,17,18-octafluoro-5,10,15,20-tetrakis(pentafluorophenyl)porphyrinato(2−), β-X_8-2,6-Cl_2tpp (X = F/Cl/Br) = 2,3,7,8,12,13,17,18-octafluoro/octachloro/octabromo-5,10,15,20-tetrakis(2,6-dichlorophenyl)porphyrinato(2−), β-X_8-F_{20}-tpp (X = F/Cl/Br) = 2,3,7,8,12,13,17,18-octafluoro/octachloro/octabromo-5,10,15,20-tetrakis(pentafluorophenyl)porphyrinato(2−), β-Br_8-tmp = 2,3,7,8,12,13,17,18-octabromo-5,10,15,20-tetrakis(2,4,6-trimethylphenyl)porphyrinato(2−), β-Ph_8-tpp = 2,3,5,7,8,10,12,13,15,17,18,20-dodecaphenylporphyrinato(2−), oep = 2,3,7,8,12,13,17,18-octaethylporphyrinato(2−), 2,4,6-$(MeO)_3$tpp = 5,10,15,20-tetrakis(2,4,6-trimethoxyphenyl)porphyrinato(2−).

[2] J. T. Groves, T. E. Nemo, R. S. Myers, *J. Am. Chem. Soc.* **1979**, *101*, 1032.

[3] a) B. Meunier, *Chem. Rev.* **1992**, *92*, 1411; b) J. P. Collman, X. Zhang, V. J. Lee, E. S. Uffelman, J. I. Brauman, *Science* **1993**, *261*, 1404; c) D. Mansuy, *Coord. Chem. Rev.* **1993**, *125*, 129.

[4] D. Dolphin, T. G. Traylor, L. Y. Xie, *Acc. Chem. Res.* **1997**, *30*, 251.

[5] C. K. Chang, F. Ebina, *J. Chem. Soc. Chem. Commun.* **1981**, 778.

[6] P. S. Traylor, D. Dolphin, T. G. Traylor, *J. Chem. Soc. Chem. Commun.* **1984**, 279.

[7] T. G. Traylor, S. Tsuchiya, *Inorg. Chem.* **1987**, *26*, 1338.

[8] a) P. E. Ellis, Jr., J. E. Lyons, *Catal. Lett.* **1989**, *3*, 389; b) P. E. Ellis, Jr., J. E. Lyons, *Coord. Chem. Rev.* **1990**, *105*, 181.

[9] P. Hoffmann, G. Labat, A. Robert, B. Meunier, *Tetrahedron Lett.* **1990**, *31*, 1991.

[10] J. F. Bartoli, O. Brigaud, P. Battioni, D. Mansuy, *J. Chem. Soc. Chem. Commun.* **1991**, 440.

[11] M. W. Grinstaff, M. G. Hill, J. A. Labinger, H. B. Gray, *Science* **1994**, *264*, 1311.

[12] a) E. Porhiel, A. Bondon, J. Leroy, *Tetrahedron Lett.* **1998**, *39*, 4829; b) E. Porhiel, A. Bondon, J. Leroy, *Eur. J. Inorg. Chem.* **2000**, 1097.

[13] F. Hino, D. Dolphin, *Chem. Commun.* **1999**, 629.

[14] E. Baciocchi, T. Boschi, L. Cassioli, C. Galli, L. Jaquinod, A. Lapi, R. Paolesse, K. M. Smith, P. Tagliatesta, *Eur. J. Org. Chem.* **1999**, 3281.

[15] F. G. Doro, J. R. L. Smith, A. G. Ferreira, M. D. Assis, *J. Mol. Catal. A* **2000**, *164*, 97.

[16] Note that under certain conditions (such as with H_2O_2 rather than PhIO as the oxidant) the β-halogenation of the phenyl-halogenated catalysts may reduce their efficiency in catalyzing hydrocarbon oxidations (see ref. [12b]). Moreover, it is reported that [Fe^{III}(β-Br_8-tmp)Cl] and [Fe^{III}(β-Cl_8-2,6-Cl_2tpp)Cl] are inferior to [Fe^{III}(tmp)Cl] and [Fe^{III}(2,6-Cl_2tpp)Cl], respectively, as catalysts for PhIO hydroxylation of ethylbenzene or cyclohexane (see: Z. Gross, L. Simkhovich, *Tetrahedron Lett.* **1998**, *39*, 8171).

[17] T. Wijesekera, A. Matsumoto, D. Dolphin, D. Lexa, *Angew. Chem.* **1990**, *102*, 1073; *Angew. Chem. Int. Ed. Engl.* **1990**, *29*, 1028.

[18] P. Bhyrappa, V. Krishnan, *Inorg. Chem.* **1991**, *30*, 239.

[19] E. R. Birnbaum, W. P. Schaefer, J. A. Labinger, J. E. Bercaw, H. B. Gray, *Inorg. Chem.* **1995**, *34*, 1751.

[20] E. K. Woller, S. G. DiMagno, *J. Org. Chem.* **1997**, *62*, 1588.

[21] In the case of β-chlorination or -bromination, a severe distortion of the porphyrin ligand could occur (see, for example, refs. [4] and [11]). Such porphyrin distortion is known to destabilize the HOMO of the porphyrin macrocycle, making the porphyrin ligand easier to oxidize (opposite to the inductive effect of the electron-withdrawing β-halogen substituents); however, the reduction of porphyrin ligands is little affected by the porphyrin distortion. See: a) M. O. Senge, in *Porphyrin Handbook, Vol. 1* (Eds.: K. M. Kadish, K. M. Smith, R. Guilard), Academic Press, San Diego, **2000**, Chapter 6, p. 239; b) K. M. Kadish, E. van Camelbecke, G. Royal, in *Porphyrin Handbook, Vol. 8* (Eds.: K. M. Kadish, K. M. Smith, R. Guilard), Academic Press, San Diego, **2000**, Chapter 55, p. 1.

[22] a) P. G. Gassman, A. Ghosh, J. Almlöf, *J. Am. Chem. Soc.* **1992**, *114*, 9990; b) A. Ghosh, *J. Am. Chem. Soc.* **1995**, *117*, 4691; c) A. Ghosh, *Acc. Chem. Res.* **1998**, *31*, 189.

[23] H. L. Chen, P. E. Ellis, Jr., T. Wijesekera, T. E. Hagan, S. E. Groh, J. E. Lyons, D. P. Ridge, *J. Am. Chem. Soc.* **1994**, *116*, 1086.

[24] a) J. T. Groves, W. J. Kruper Jr., *J. Am. Chem. Soc.* **1979**, *101*, 7613; b) S. E. Creager, R. W. Murray, *Inorg. Chem.* **1985**, *24*, 3824; c) J. M. Garrison, T. C. Bruice, *J. Am. Chem. Soc.* **1989**, *111*, 191; d) J. M. Garrison, D. Ostovic, T. C. Bruice, *J. Am. Chem. Soc.* **1989**, *111*, 4960.

[25] a) J. T. Groves, R. C. Haushalter, M. Nakamura, T. E. Nemo, B. J. Evans, *J. Am. Chem. Soc.* **1981**, *103*, 2884; b) S. Tsuchiya, *J. Chem. Soc. Chem. Commun.* **1991**, 716; c) K. Yamaguchi, Y. Watanabe, I. Morishima, *J. Chem. Soc. Chem. Commun.* **1992**, 1721; d) H. Fujii, *J. Am. Chem. Soc.* **1993**, *115*, 4641; e) Z. Gross, S. Nimri, *J. Am. Chem. Soc.* **1995**, *117*, 8021; f) Y. M. Goh, W. Nam, *Inorg. Chem.* **1999**, *38*, 914.

[26] a) J. T. Groves, W. J. Kruper, Jr., R. C. Haushalter, *J. Am. Chem. Soc.* **1980**, *102*, 6375; b) M. Schappacher, R. Weiss, *Inorg. Chem.* **1987**, *26*, 1189; c) J. T. Groves, M. K. Stern, *J. Am. Chem. Soc.* **1987**, *109*, 3812; d) J. T. Groves, M. K. Stern, *J. Am. Chem. Soc.* **1988**, *110*, 8628; e) R. D. Arasasingham, G.-X. He, T. C. Bruice, *J. Am. Chem. Soc.* **1993**, *115*, 7985.

[27] a) J. T. Groves, R. Quinn, *J. Am. Chem. Soc.* **1985**, *107*, 5790; b) W.-H. Leung, C.-M. Che, *J. Am. Chem. Soc.* **1989**, *111*, 8812; c) C. Ho, W.-H. Leung, C.-M. Che, *J. Chem. Soc. Dalton Trans.* **1991**, 2933; d) T.-S. Lai, R. Zhang, K.-K. Cheung, H.-L. Kwong, C.-M. Che, *Chem. Commun.* **1998**, 1583; e) C.-J. Liu, W.-Y. Yu, S.-M. Peng, T. C. W. Mak, C.-M. Che, *J. Chem. Soc. Dalton Trans.* **1998**, 1805; f) C.-J. Liu, W.-Y. Yu, C.-M. Che, C.-H. Yeung, *J. Org. Chem.* **1999**, *64*, 7365.

[28] We notice that a β-halogenated oxoiron(IV) porphyrin radical cation, [Fe^{IV}(β-Cl_8-$tmp^{\bullet+}$)(O)], has been generated in CH_2Cl_2 at −80 °C, but the reactivity of this oxoiron species toward hydrocarbon oxidations is not reported (see: P. Ochsenbein, D. Mandon, J. Fischer, R. Weiss, R. Austin, K. Jayaraj, A. Gold, J. Terner, E. Bill, M. Müther, A. X. Trautwein, *Angew. Chem.* **1993**, *105*, 1504; *Angew. Chem. Int. Ed. Engl.* **1993**, *32*, 1437).

[29] J. R. Bryant, J. M. Mayer, *J. Am. Chem. Soc.* **2003**, *125*, 10351.

[30] a) M. Tsutsui, D. Ostfeld, L. M. Hoffman, *J. Am. Chem. Soc.* **1971**, *93*, 1820; b) J. J. Bonnet, S. S. Eaton, G. R. Eaton, R. H. Holm, J. A. Ibers, *J. Am. Chem. Soc.* **1973**, *95*, 2141; c) G. M. Brown, F. R. Hopf, J. A. Ferguson, T. J. Meyer, D. G. Whitten, *J. Am. Chem. Soc.* **1973**, *95*, 5939; d) R. G. Little, J. A. Ibers, *J. Am. Chem. Soc.* **1973**, *95*, 8583; e) D. P. Rillema, J. K. Nagle, L. F. Barringer, Jr., T. J. Meyer, *J. Am. Chem. Soc.* **1981**, *103*, 56; f) J. P. Collman, C. E. Barnes, P. N. Swepston, J. A. Ibers, *J. Am. Chem. Soc.* **1984**, *106*, 3500.

[31] a) S.-I. Murahashi, T. Naota, N. Komiya, *Tetrahedron Lett.* **1995**, *36*, 8059; b) J. T. Groves, M. Bonchio, T. Carofiglio, K. Shalyaew, *J. Am. Chem. Soc.* **1996**, *118*, 8961.

[32] a) S. S. Eaton, G. R. Eaton, *J. Am. Chem. Soc.* **1975**, *97*, 3660; b) J. T. Groves, R. Quinn, *Inorg. Chem.* **1984**, *23*, 3844.

[33] a) W.-C. Lo, C.-M. Che, K.-F. Cheng, T. C. W. Mak, *Chem. Commun.* **1997**, 1205; b) A. Berkessel, M. Frauenkron, *J. Chem. Soc. Perkin Trans. 1* **1997**, 2265; c) T.-S. Lai, H.-L. Kwong, R. Zhang, C.-M. Che, *J. Chem. Soc. Dalton Trans.* **1998**, 3559.

[34] E. R. Birnbaum, W. P. Schaefer, J. A. Labinger, J. E. Bercaw, H. B. Gray, *Inorg. Chem.* **1995**, *34*, 1751.

[35] The ν(CO) frequencies of previously reported carbonylruthenium(II) *meso*-tetraarylporphyrin complexes fall in the range of 1918–1990 cm^{-1}, see: a) references [30–34]; b) J. P. Collman, C. E. Barnes, P. J. Brothers, T. J. Collins, T. Ozawa, J. C. Gallucci, J. A. Ibers, *J. Am. Chem. Soc.* **1984**, *106*, 5151; c) C. Slebodnick, K. Kim, J. A. Ibers, *Inorg. Chem.* **1993**, *32*, 5338; d) B. Scharbert, E. Zeisberger, E. Paulus, *J. Organomet. Chem.* **1995**, *493*, 143; e) C. Slebodnick, W. K. Seok, K. M. Kim, J. A. Ibers, *Inorg. Chim. Acta* **1996**, *243*, 57; f) R. Salzmann, C. J. Ziegler, N. Godbout, M. T. McMahon, K. S. Suslick, E. Oldfield, *J. Am. Chem. Soc.* **1998**, *120*, 11323.

[36] Structurally characterized metal complexes bearing F_{28}-tpp ligand are sparse, see, for example: a) V. V. Smirnov, E. K. Woller, S. G. DiMagno, *Inorg. Chem.* **1998**, *37*, 4971; b) A. P. Nelson, S. G. DiMagno, *J. Am. Chem. Soc.* **2000**, *122*, 8569; c) H. Sun, V. V. Smirnov, S. G. DiMagno, *Inorg. Chem.* **2003**, *42*, 6032; d) S.-W. Lai, Y.-J. Hou, C.-M. Che, H.-L. Pang, K.-Y. Wong, C. K. Chang, N. Zhu, *Inorg. Chem.* **2004**, *43*, 3724.

[37] The coordination of water rather than methanol molecule to ruthenium in **1c**·4H_2O·MeOH is surprising, since previously reported structurally characterized carbonylruthenium(II) porphyrin complexes crystallized from alcohol-containing solvents exclusively bind an alcohol molecule at an axial site (see refs [30b] and [33a]).

[38] a) J. T. Groves, Y. Han, D. V. Engen, *J. Chem. Soc. Chem. Commun.* **1990**, 436; b) P. Le Maux, H. Bahri, G. Simonneaux, L. Toupet, *Inorg. Chem.* **1995**, *34*, 4691; c) P. G. Jene, J. A. Ibers, *J. Porphyrins Phthalocyanines* **2001**, *5*, 419.

[39] Note that [Ru^{II}(β-Ph_8-tpp)(CO)(Py)], a β-phenylated carbonylruthenium(II) porphyrin with a severely saddle-distorted porphyrin ligand, has a long Ru–C(CO) bond of 1.93(1) Å (see ref. [27e]), which is comparable with the Ru–C(CO) bond in **1b**·H_2O·2CH_2Cl_2. The carbonyl iron(II) porphyrin [Fe^{II}(tpp)(CO)(1-MeIm)] (1-MeIm = 1-methylimidazole) was reported to have a short C–O bond of 1.061(3) Å (ref. [35f]), coupled with a normal Fe–C(CO) bond of 1.793(3) Å.

[40] K. M. Kadish, Y. Hu, X. H. Mu, *J. Heterocycl. Chem.* **1991**, *28*, 1821.

[41] Such interporphyrin CO···L hydrogen bonds in a [Ru^{II}(por)(CO)]·L complex that generate polymeric one-dimensional chain structures have not been observed before. We notice that [Ru^{II}(oep)(CO)]·H_2O also shows interporphyrin hydrogen-bonding, but the hydrogen-bonding is only between the coordinated water molecules, leading to formation of hydrogen-bonded porphyrin dimers with much longer $O(H_2O)\cdots O(H_2O\cdot)$ distances of 3.07 Å (see ref. [40]).

[42] T. C. W. Mak, C.-M. Che, K.-Y. Wong, *J. Chem. Soc. Chem. Commun.* **1985**, 986.

[43] a) R. G. Ball, G. Domazetis, D. Dolphin, B. R. James, J. Trotter, *Inorg. Chem.* **1981**, *20*, 1556; b) S. Ariel, D. Dolphin, G. Domazetis, B. R. James, T. W. Leung, S. J. Rettig, J. Trotter, G. M. Williams, *Can. J. Chem.* **1984**, *62*, 755; c) E. Stulz, M. Maue, N. Feeder, S. J. Teat, Y.-F. Ng, A. D. Bond, S. L. Darling, J. K. M. Sanders, *Inorg. Chem.* **2002**, *41*, 5255.

[44] For example, the reactions of **2b**,**c** with styrene exhibited isosbestic points at 405, 430 nm for **2b** and 396, 480 nm for **2c**. In the absence of pyrazole, no isosbestic points were observed.

[45] We found that the rate constants obtained are not dependent on the concentration of pyrazole present in the reaction mixtures. For example, varying the concentration of pyrazole within the range of 1–10% w/w did not cause appreciable change in the rate constants. In the absence of hydrocarbon substrates, the dioxo complexes **2a–f** exhibit no appreciable reaction with pyrazole under the same conditions on the time scale of the kinetic studies.

[46] J.-L. Zhang, C.-M. Che, *Chem. Eur. J.* **2005**, *11*, 3899.

[47] J. Leroy, A. Bondon, L. Toupet, *Acta Crystallogr. Sect. C* **1999**, *55*, 464.

[48] a) J. Leroy, A. Bondon, L. Toupet, C. Rolando, *Chem. Eur. J.* **1997**, *3*, 1890; b) V. V. Smirnov, E. K. Woller, D. Tatman, S. G. DiMagno, *Inorg. Chem.* **2001**, *40*, 2614.

[49] X.-K. Jiang, *Acc. Chem. Res.* **1997**, *30*, 283.

[50] L. K. Stultz, M. H. V. Huynh, R. A. Binstead, M. Curry, T. J. Meyer, *J. Am. Chem. Soc.* **2000**, *122*, 5984.

[51] K. A. Gardner, L. L. Kuehnert, J. M. Mayer, *Inorg. Chem.* **1997**, *36*, 2069.

[52] J. Kaizer, E. J. Klinker, N. Y. Oh, J.-U. Rohde, W. J. Song, A. Stubna, J. Kim, E. Münck, W. Nam, L. Que Jr., *J. Am. Chem. Soc.* **2004**, *126*, 472.

[53] H. Lindler, R. Dubuis, *Org. Synth. Collect.* **1973**, *5*, 880.

[54] a) R. L. Halterman, S.-T. Jan, *J. Org. Chem.* **1991**, *56*, 5253; b) R. L. Halterman, S.-T. Jan, H. L. Nimmons, D. J. Standlee, M. A. Khan, *Tetrahedron* **1997**, *53*, 11257.

Received: July 15, 2005
Published online: September 15, 2005

